STUDYING THE OXYFUEL COMBUSTION SYSTEM'S ABILITY TO SPONTANEOUSLY BURN PULVERIZED COAL

Bhaskar.B, Katti,Rajesh.J, Murthy.S.L
Asst. Prof, Asst. Prof, Asst. Prof
bbkatti@pdit.ac.in, rajeshjavali@gmail.com, murthypdit@gmail.com
Department of Mechanical, Proudhadevaraya Institute of Technology, Abheraj Baldota Rd, Indiranagar, Hosapete, Karnataka-583225

Abstract
Combustion of coal produces around 40% of the world's electricity; it is also the most plentiful energy source. Coal burning could not provide as much electricity because of the pollution it caused. To use the vast energy of coal for electricity generation, its emissions must be reduced. In order to decrease emissions from coal-fired furnaces, a thorough comprehension of different parts of coal combustion is necessary. This paper's goal is to provide a comprehensive overview of pulverised coal combustion techniques, including oxy-fuel combustion, coal and biomass co-combustion, pulverised coal boiler emissions, ash production and deposition, carbon capture, and more.

and codon sequestration (CCS) technology to detail the advancements achieved in these areas. This review covers both numerical and experimental elements. Also included in this overview are the thermodynamics of the combustion process. Also included in this study is an investigation into how several submodels, including those for devolatilization, char combustion, radiation, and turbulent combustion, impact the combustion process of pulverised coal.

KEYWORDS
biomass, CCS, CFD, combustion, devolatilization, emission, pulverized coal

1 | INTRODUCTION

Electricity demand is increasing worldwide, and power generation relies on fossil fuel specifically on coal. It is supposed that the need for power production will grow in upcoming decades as population tends to increase, which will increase the demand for electricity by the use of more electrically powered devices. Fossil fuels will continue being dominant energy production source as coal reserves are abundant worldwide. Approximately 80% coal reserves are in 10 countries. The USA tops the list with around 25% of total coal reserves. Table 1 shows the total proved coal reserves and reserve to production ratio at the end of 2017.

Power production by the combustion of coal produces greenhouse gases emission. CO_2 is the primary contributor of greenhouse gases emission produced by coal combustion. According to the International Energy Agency (IEA 2015), fossil fuel combustion produces half of the total CO_2 emission. Coal needs to be burned in a

ISSN NO: 9726-001X
Volume 10 Issue 03 2022

TABLE 1 Total proved coal reserves at the end of 2017[142]

Country	Coal Reserves (Million Tonnes)	Share of Total (%)	Reserves to Production Ratio
USA	250 916	24.2	357
Russian Federation	160 364	15.5	391
Australia	144 818	14	301
China	138 819	13.4	39
India	97 728	9.4	136
Germany	36 108	3.5	206
Ukraine	34 375	3.3	*
Poland	25 811	2.49	203
Kazakhstan	25 605	2.47	230
Indonesia	225 598	2.2	49
Turkey	11 353	1.1	115
South Africa	9893	1	39

manner, not to emit greenhouse gases, NO_x, SO_x, and particulate matter more than the environmentally acceptable limit.

The mechanism of pulverized coal combustion is extremely complicated, in which interaction of carbonaceous and mineral components, with gaseous phase, takes place. Barnes[1] presented the mechanism involved in pulverized fired coal combustion as shown in Figure 1. Coal particles entering the combustion chamber are subjected to a very high temperature at 1500°C, and heating rate a million degree per second. Carbonaceous components and mineral matters undergo a highly aggressive time-temperature profile, due to which a large number of reactions takes place.

Many reviews focussing on oxy-fuel combustion and co-combustion of coal and biomass are available in the literature. Chen et al[2] presented details of oxy-fuel combustion including characterizations, fundamentals of combustion processes, and CFD modeling techniques. They focused on the basic principles of pulverized coal

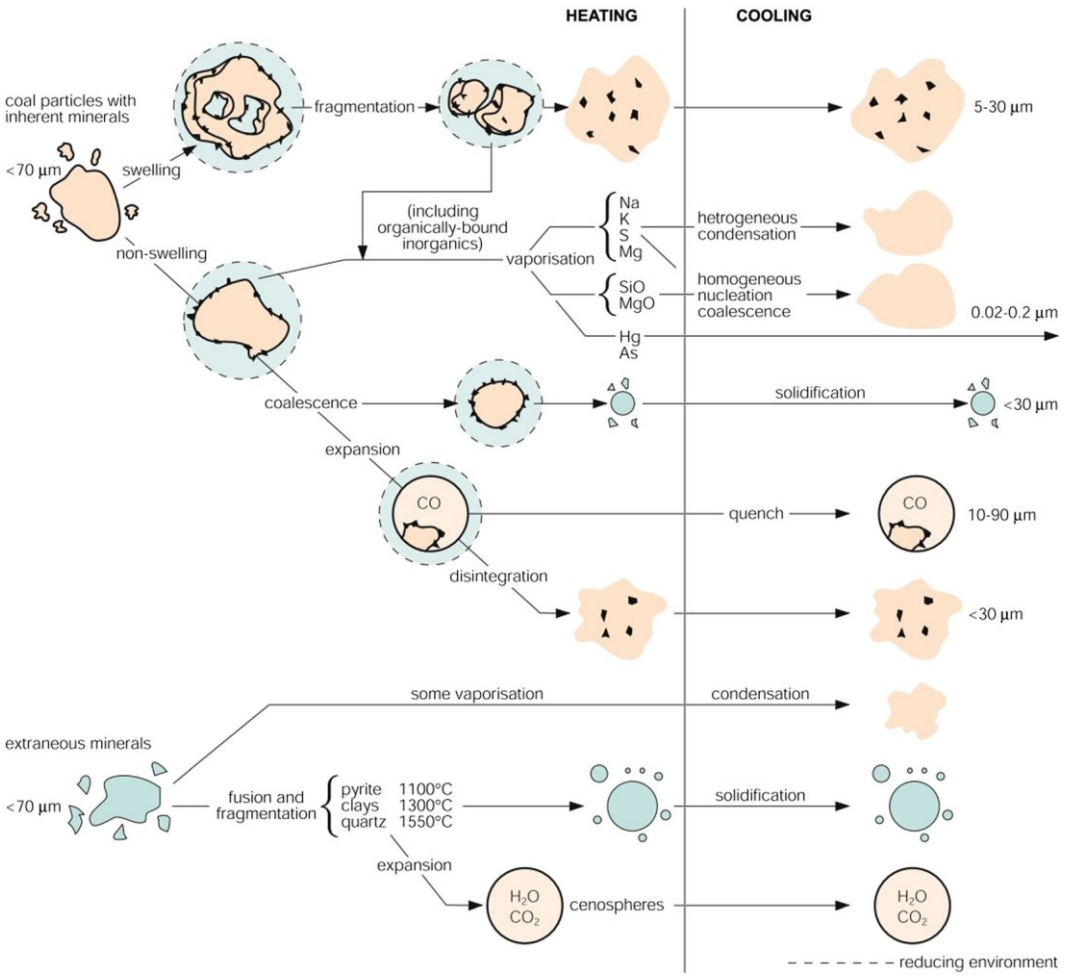

FIGURE 1 Summary of main ash forming mechanisms during pulverized coal combustion[1] [Colour figure can be viewed at wileyonlinelibrary.com]

combustion in the oxy-fuel atmosphere. They explored the difference between oxy-fired combustion and air-fired combustion by considering parameters such as heat transfer, slurry atomization, fuel delivery, the interaction of particle phase with the gas phase, flame stabilization, and pollutant formation. Along with the review of experimental and numerical studies, they explored the impact of diluting medium on combustion processes. Scheffknecht et al[3] presented oxy-fuel combustion review emphasizing on flame characterization, NO_x emission, modeling of oxy-fuel combustion including reaction submodels, and heat transfer submodels. Edge et al[4] tried to summarize the available advance computer modeling approaches for the oxy-fuel combustion and focused on submodels for key combustion processes such as coal devolatilization char combustion, turbulence, radiation, and pollutant emission. Wall et al[5] presented a review to explore the science underpinning oxy-fuel combustion technology. They outlined the development of research and technology in oxy-fuel combustion by joint Australia-Japan feasibility project. They explored the difference between conventional combustion and oxy-fuel combustion in terms of coal reactivity, heat transfer, and pollutant emission. Yin and Yan[6] presented a review on combustion fundamentals and modeling of pulverized fired oxy-fuel plants. They addressed the fundamentals and modeling of pulverized fuel oxy-fuel combustion technology. They focused on combustion chemistry such as coal devolatilization and char combustion along with the interaction of particle phase with gaseous phase, heat and mass transfer, and how these parameters are affected in oxy-fuel combustion conditions. They further investigated modeling and implementation of these parameters into CFD simulation. Tabet and Gökalp[7] addressed the modeling approaches based on CFD for the prediction of co-combustion characteristics of pulverized coal and biomass under oxy-fired and air fired combustion atmosphere. They presented a thorough overview of submodels required for the prediction of co-combustion characteristics under oxy-fuel and air combustion conditions. Agbor et al[8] reviewed biomass co-firing with coal focusing on various co-firing technologies, feasible strategies for the improvement of biomass co-firing for the future development of co-firing in North America and around the world. Nemitallah et al[9] reviewed the current status and future trends of oxy-fuel combustion technology and focused on its application in existing combustion systems and novel oxygen transport reactors (OTR). They discussed the required modification in existing conventional combustion system for retrofitting. They also performed a techno-economic analysis of oxy-combustion integrated combustion system. Mathekga et al[10] reviewed the existing literature of fluidized bed combustion in the oxy-fuel environment. They mainly focused on char combustion, heat transfer, and pollutant emission in their review. They also discussed the modeling aspects of fluidized bed boilers in the oxy-fuel atmosphere. Borah et al[11] presented current state of art on coal devolatilization in fluidized bed gasification and combustion. They emphasized the improvement of coal gasification and combustion efficiency. They also explained the effect of volatile matter in coal on fluidized bed combustion which will be helpful for the design and control of fluidized bed combustors for high volatile coals. Habib et al[12] presented a detailed overview of CCS technologies paying special attention to oxy-fuel combustion process utilizing ion-transport membranes (ITM) for O_2 separation. They reviewed existing literature on the performance of oxy-fuel combustion and its potential for carbon capture and sequestration (CCS) in membrane reactors.

The aim of present paper is to provide a comprehensive and up-to-date review of various aspects of coal combustion such as oxy-fuel combustion, co-combustion of coal and biomass, emissions from pulverized coal furnaces, ash formation and deposition, CCS technologies etc., which will be useful for newcomers and researchers in this field to realize the potential research gap. The specific objectives of this paper are (1) to outline the progress made in various coal combustion aspects, (2) to summarize the effect of various submodels such as devolatilization model, char combustion model, radiation model, and turbulence model on the pulverized coal combustion process and discusses their pros and cons, (3) to present a brief discussion on thermodynamic aspects of pulverized coal combustion such as thermodynamic irreversibility and exergy loss during the combustion process, (4) to explore the instruments which are necessary for experimental work, used by various authors, and (5) to present a discussion on opportunities, challenges, and future need in the field of pulverized coal combustion.

The remaining paper is organized as follows. Section 2 of the paper presents fundamental aspects of coal combustion processes. Experimental and numerical aspects of pulverized coal combustion are considered to address the combustion phenomenon of pulverized coal. These aspects include combustion under oxy-fuel combustion, co-combustion of coal and biomass, thermodynamic aspects of coal combustion, CCS technologies, and numerical modeling of combustion processes. The effect of various submodels such as turbulence, radiation, devolatilization, and char combustion on pulverized coal combustion is also discussed. Section 3 includes the complete details of experimental instruments used by various authors for their work, and in

ISSN NO: 9726-001X
Volume 10 Issue 03 2022

Section 4 challenges, opportunities, and future research directions are discussed.

2 | ASPECTS OF COAL COMBUSTION

2.1 | Oxy-fuel combustion

Emission of greenhouse gases will be a primary environmental concern since coal will be the principal energy resource for the power production for upcoming decades. Capture and storage of greenhouse gases are necessary for the mitigation of greenhouse gas emissions. During the past few years, combustion of fuel under oxy-fired combustion environment has gained a lot of attention due to the capability of CO_2 capture.

Figure 2 shows the conventional air blown power plant. In conventional air-fired combustion, nitrogen dilutes combustion products such as CO_2 and water vapor in the flue gas. In oxy-fuel combustion power plant as shown in Figure 3, pure oxygen (having around 95% purity) and recycled flue gas (RFG) is used for combustion. Recycled flue gas (RFG) works as diluents and controls the flame temperature in the oxy-fired power plant. The exhaust gas generated has mainly CO_2 and water vapor. The highly concentrated CO_2 can be easily separated by condensing water vapor.

Oxy-fuel combustion has unstable flame, delayed flame ignition, low flame temperature, changed heat transfer, and decreased NO_x and SO_x emission than the air combustion. These differences in performance of oxy-fuel combustion are due to different properties of CO_2 than N_2 as shown in Table 2. CO_2 has higher molar heat capacity than N_2; thus, CO_2 can work as a better heat sink than N_2. It is the main reason behind reduced flame temperature in the oxy-fuel environment. CO_2 has higher molecular weight than N_2 which results into highly dense flue gas in oxy-fuel conditions and causes lower gas velocity and higher residence time of particles in the furnace. Slower flame propagation speed in oxy-fuel condition is due to lower thermal diffusivity of CO_2. The combustion gases have lower temperature under oxy-fired conditions than the air-fired conditions at identical O_2 content due to higher energy per volume of CO_2. The RFG has high partial pressure which causes higher flue gas emittance. Thus, to obtain identical radiative heat transfer in boiler retrofitted to oxyfuel, O_2 content should be less than the required levels for the same AFT in O_2/RFG passing through the burner.[14]

2.1.1 | Flame characterization, ignition, and burnout

Hees et al[15] compared the air flames and the flame produced under the oxy-fuel atmosphere in term of radical

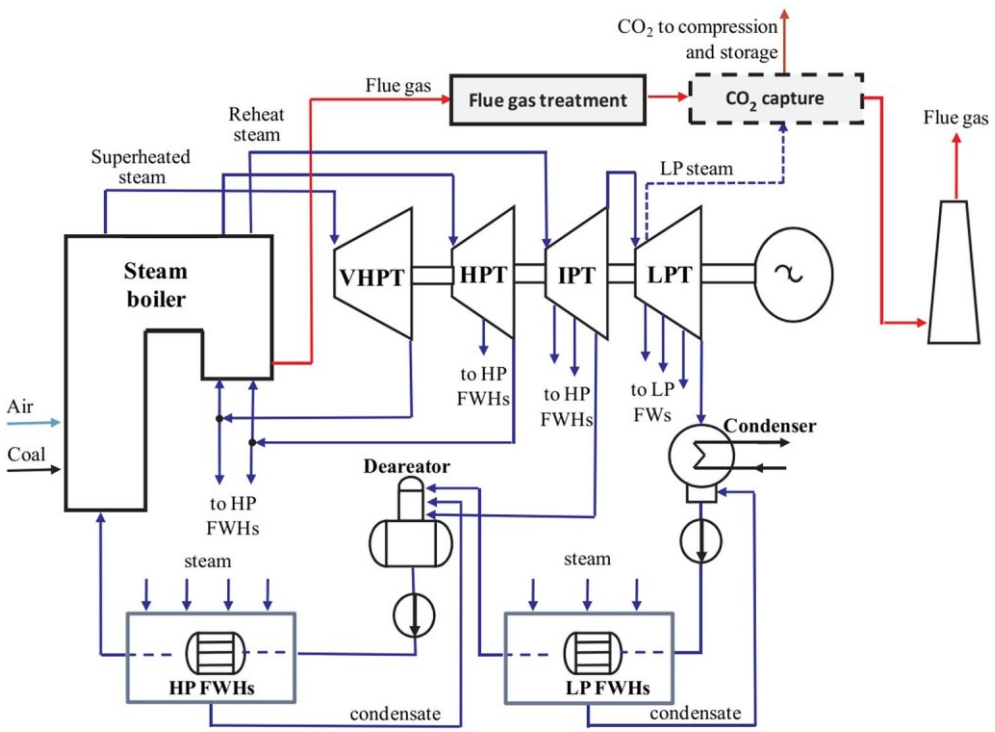

FIGURE 2 Schematic of air-fired power plant[13] [Colour figure can be viewed at wileyonlinelibrary.com]

ISSN NO: 9726-001X
Volume 10 Issue 03 2022

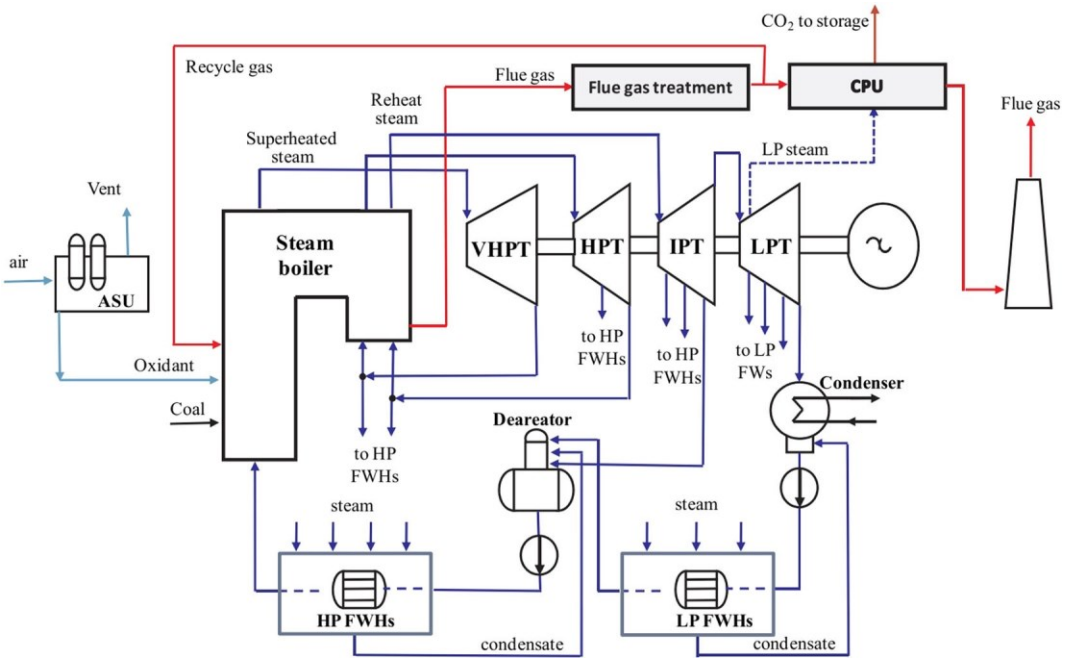

FIGURE 3 Schematic of oxy-fired power plant[13] [Colour figure can be viewed at wileyonlinelibrary.com]

TABLE 2 Gas properties for N_2 and CO_2 at 1173K[14]

Property	N_2	CO_2	Ratio CO_2/N_2
Thermal conductivity (W/m-K)	0.07467	0.08169	1.09
Molar heat capacity (kJ/kmol-K)	33.6	56.1	1.67
Density (kg/m^3)	0.29	0.45	1.55
O_2 diffusion coefficient (m^2/s)	3.074e − 04	2.373e − 04	0.77
Thermal diffusivity (m^2/s)	2.167e − 04	1.420e − 04	0.65
Molecular weight (kg/kmol)	28	44	1.57
Energy per volume (J/m^3-K)	0.34	0.57	1.67

activity of excited OH radicals. Spontaneously emitted excited OH radicals were captured by CCD camera. They found air flames more radiant than oxy-fired flames at identical O_2 concentration. They observed short and wide flames by varying local oxygen fuel ratio from 1.0 to 0.6 at a fixed global oxygen-fuel ratio of 1.3. Hjärtstam et al[16] experimentally described the oxy-fuel flame structure of lignite coal in three different cases which were obtained by varying flue gas RR and compared with the flames obtained under the conventional air-fired case. They found reduced flame temperature in the oxy-fired case than in air-fired combustion environment. Higher heat capacity of CO_2 was the major reason behind reduced flame temperature in the oxy-fired conditions. Hence, to obtain flame temperature identical to air fired environment, they increased oxygen concentration to 25% in the oxy-fuel environment. Further increase in oxygen concentration to 27% and 29%, the flame temperature increases by 50°C and 100°C, respectively, in the oxy-fuel atmosphere. Toporov et al[17] performed flame stability analysis and inflame measurements of continuous phase velocity and temperature in a 100-kW vertical pilot-scale furnace in O_2/N_2 and O_2/CO_2 combustion environment. They observed reduced flame stability and poor burnout in 21% O_2/79% CO_2 combustion condition. To overcome the flame stability issue in the oxy-fuel combustion, they redesigned the burner and increased secondary stream swirl which strengthens the IRZ. Jovanović et al[18] proposed a novel LES model able to handle all possible ignition/combustion mechanism of pulverized coal particles in oxy-fuel combustion and solved ignited jet flame of pulverized coal using proposed model. They addressed limitations of the standard k-ε model by comparing the performance of the proposed model with the standard model. The proposed model accurately predicted flame properties such as flame stability, flame shape, ignition

ISSN NO: 9726-001X
Volume 10 Issue 03 2022

position, and luminosity. Their proposed model accurately predicted ignition temperature for all oxygen fractions within 5% error. Riaza et al[19] measured ignition temperature, burnout, and NO emission in an entrained flow reactor under oxy-fired condition by blending coal of different rank with olive waste. They reported the increase in ignition temperature and reduction in burnout value under the oxy-fired condition having 21% O_2. When the O_2 concentration was increased to 30% to 35%, ignition temperature reduces and burnout improves. Reduction in ignition temperature and improvement in burnout can be found by adding biomass to coal. This trend becomes more evident with increasing biomass content. Burnout is also depending on equivalence ratio and decreases with increase in equivalence ratio as the availability of oxygen reduces at higher fuel equivalence ratio. Increase in burnout during co-firing is also reported by Smart et al.[20] Ignition behavior and burnout performance were studied by Bhuiyan and Naser[21] under the oxy-fired environment in 550 MW tangentially fired furnace firing coal with biomass. They observed improved burnout during co-firing in the oxy-fuel environment. As char particle temperature in the oxy-fuel atmosphere is less than conventional air combustion condition, Zhou et al[22] attempted to adjust char particle temperature in oxy-fuel condition to that were in air combustion by replacing some part of CO_2 with Ar (molar heat capacity of Ar < N_2 < CO_2). Liu et al[23] presented a numerical simulation of oxy-fired pulverized coal boiler focussing on the effect of swirl number, flue gas recycle ratio, blockage ratio and oxygen partial pressure on flame stability, shape, type, and structure. They found improved flame stability due to internal recirculation zone whereas oxy-coal flame was destroyed by the central dark primary core. They reported that the volume of the dark primary core was affected more by the swirl number and recycle ratio than the other two factors. Chae et al[24] evaluated the performance of 30 MW oxy-fuel retrofitted tangential vane swirl burner. They investigated the effect of main design parameters on the flame characteristics. They reported that the flame characteristics were strongly affected by O_2 concentration present in the primary oxidizer. They further added that the decrease in O_2 concentration in primary oxidizer resulted into increase in flame length, which was the major cause of delayed ignition near the fuel nozzle. Identical O_2 concentration in both primary and secondary oxidizer provided favorable combustion conditions.

2.1.2 | Heat transfer under oxy-fuel combustion

Heat transfer characteristics of pulverized coal change significantly when combustion environment is altered to oxyfuel from conventional air combustion environment. The change in heat transfer characteristics in oxyfuel environment is attributed due to increase in CO_2 and H_2O concentration along with the increased concentration of particulate media such as char, fly ash, and so on.[14] Heat transfer characteristics in oxy-fuel combustion conditions are investigated in laboratory, pilot, and demonstration scale furnaces by various authors.

Smart et al[25] measured radiative and convective heat flux during co-combustion of biomass with coal under oxy-fuel combustion conditions at various recycle ratio. Their result showing the highest radiative flux and highest luminosity the lowest RR is shown in Figure 4. They reported that the biomass addition to coal has a negative effect on radiation heat transfer. They further added that the highest convective flux corresponded to lowest radiative flux. Guo et al[26] investigated the oxy-fuel combustion characteristics of sub-bituminous coal in 35 MW large scale boiler. They measured furnace temperature, the concentration of species, exhaust gas emissions, and heat transferred to superheater and membrane wall in

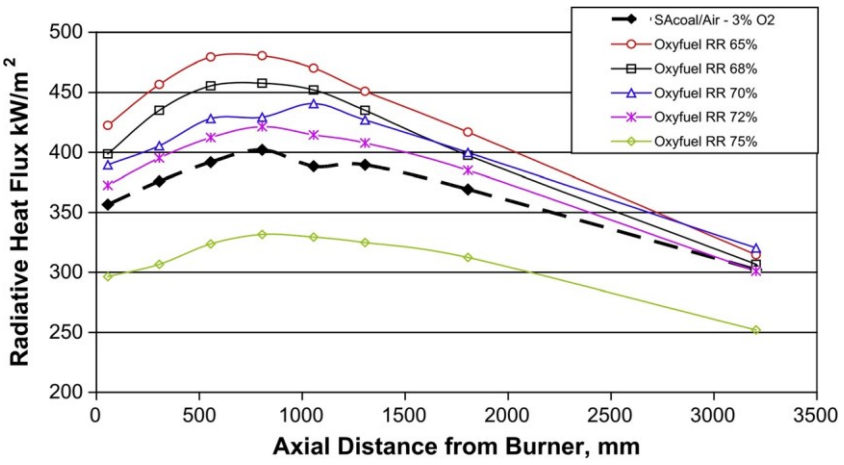

FIGURE 4 Effect of recycle ratio (RR) on radiative heat flux[25] [Colour figure can be viewed at wileyonlinelibrary.com]

oxy-fuel (both wet and dry recycling) and air-fired condition. They obtained identical mean temperature and heat flux distribution in dry and wet FGR oxy-fuel conditions for an initial oxygen concentration of 28%. Under oxy-fuel combustion condition, heat transferred to membrane wall and superheater was slightly greater than that obtained under air combustion. They further reported that heat transfer in oxy-fuel combustion environment is influenced by flue gas recycle ratio. They obtained a reduction in heat transferred to the membrane wall and increase in superheater by 6% and 4%, respectively, when the recycle ratio was increased from 0.71 to 0.73. Rebola and Azevedo[27] numerically investigated combustion characteristics of pulverized coal in the air and oxy-fuel combustion environment emphasizing on wall incident heat flux. They compared computational results with experimental data obtained in 0.5 MW combustion test facility. They assumed flow as axisymmetric and dealt particle phase simulation with the well-known Lagrangian method. They observed that the RR 72 had identical incident heat flux to air firing combustion condition. They further showed the increase in incident heat flux and reduction in absorbed heat flux by 10% and 7%, respectively, when wall temperature is increased by 3°C. According to them, incident wall heat fluxes show higher dependency on wall temperature than recycle ratio.

Nakod et al[28] performed CFD simulations using both gray and non-gray radiation modeling approach in full scale and lab scale furnaces. They performed combustion in oxy-fuel conditions (both wet and dry flue gas recycling) and conventional air-fired condition. They found reasonable agreement in temperature profile with experimental data. The difference in temperature profile and radiative flux predicted by gray and non-gray WSGGM was minimized due to reduced flame temperature and shorter path length in lab scale furnace. Greater flame temperature and longer path length in large-scale boiler caused around 10% difference in radiative flux and 40 to 50 K difference in mean outlet gas temperature. Silva and Krautz[29] conducted heat transfer studies in 0.4 MW test facility employing staged feed gas burner. They correlated heat transfer in terms of swirl number and flow ratios. They reported that adiabatic flame temperature is a strong function of oxygen concentration, water vapor concentration, feed gas temperature, and stoichiometric ratio. They further showed that similar value of adiabatic flame temperature was obtained at 31% O_2 concentration. They reported the reduction in peak temperature in the oxy-fuel environment due to less temperature of feed gas and the larger proportion of CO_2 and water vapor in the furnace. Based on the study, they concluded that heat transfer is affected by feed gas distribution and swirl strength in the furnace. Li et al[30] performed CFD modeling of 600 MW tangentially fired boiler. They investigated the combustion and heat transfer characteristics for various oxygen volume fraction in both dry and wet recycle modes. They found total heat transfer rate identical to air-fired combustion at 27% and 28.3% oxygen volume fraction for wet and dry recycle, respectively.

2.2 | Co-combustion of coal and biomass

As sources of fossil fuels are depleting day by day, co-combustion of coal and biomass can be promoted for effective utilization of biomass and waste. Combustion of biomass with coal increases the use of renewable biomass for the generation of electric power and save capital cost by utilizing existing power plants.[8] Co-combustion of coal and biomass also serves as a cheap, renewable, and sustainable energy alternative and assures the decreased NO_x, SO_x, and CO_2 emissions.[31] Co-combustion also offers operation in flexible mode (proportion of secondary fuels can be varied). Biomass fuels have higher volatile matter thus can be utilized with low volatile coal effectively for the co-firing purpose. The nitrogen and sulfur content of biomass is lower than coal. Thus, co-combustion of coal and biomass produces little amount of SO_2 and NO_x. Co-combustion of coal and biomass reduces SO_2 emission by 75%. Level of CO_2 in the environment can be balanced by growing plants for biomass fuels. Plants extract atmospheric CO_2 during their growth. Thus, co-combustion of biomass with coal reduces CO_2 emission as the removal of CO_2 takes place from the air during the balance.[32]

2.2.1 | Flame characteristics, ignition, and burnout

Pollutant formation and burnout during solid fuel combustion are strongly dependent on flame stability and ignition behavior. Both homogeneous and heterogeneous ignition occur during solid fuel combustion. In homogeneous ignition, release of volatiles from coal particle takes place, whereas in heterogeneous ignition, oxidant directly attacks on the surface of fuel/char. The size of the biomass particle is larger than coal particles, thus, making its grinding difficult and expansive. The difference in fuel properties and particle size during co-combustion affects ignition performance and flame characteristics.

Bhuiyan and Naser[21] co-fired coal with biomass employing CFD simulation in 550 MW boiler and reported that peak temperature reduced by increasing biomass sharing as the calorific value of biomass was less than coal. Ignition and burnout temperature of sugarcane

bagasse and bamboo was investigated by Lu and Chen[33] at heating rates of 5, 10, 20, 30, and 40°C min^{-1} using TGA. Ignition temperature was evaluated by adopting intersection method (IM) and deviation method (DM), whereas they employed IM and conversion method (CM) for burnout temperature. They reported that an increase in the heating rate raised the biomass ignition and burnout temperature using IM and CM method. They observed a remarkable thermal lag in biomass particles due to the higher heating rates. Based on their investigation, they suggested a heating rate between 20°C and 30°C per min in TGA. Co-combustion characteristics of coal with bamboo, torrefied bamboo, and their blends were investigated by Liu et al.[34] They mixed bamboo and torrefied bamboo into the coal in the proportion of 10%, 20%, 30%, 40%, and 50%. On the basis of increased peak temperature and decreased weight loss rate, they reported that the reactivity of torrefied bamboo is lower than bamboo. They observed that air flow has the potential to enhance the combustion reaction and increase combustion efficiency of blends. The combustion behavior of coal and blends is studied by Moon et al[35] employing a laboratory-scale slit burner. They reported that the ignition temperature of blends has the dependency on low-rank coal, whereas burnout temperature has the dependency on high-rank coal. They reported the existence of three reaction regions in pulverized coal flames as preheating zone, zones of volatile matter reaction, and char reaction. Reaction zone's length was influenced by the fuel ratio. The co-combustion behavior of coal and biomass was investigated by Sarkar et al[36] employing TGA and DTF. They blended a substantial amount of sawdust with coal in their study. They obtained superior performance with respect to ignition index, DTF-burn out efficiency, and TGA-reactivity indices. They further added that sawdust char is more effective as co-fuel than its raw counterpart. They recommended sawdust char as a preferred option based on its operational ease and higher heat content. Elorf et al[37] presented the influence of inlet swirl on the flow field and combustion characteristics of pulverized olive cake. They considered three cases in their study: air flow without swirl, axial flow with swirl, and axial and co-axial jets with the swirl. They reported that the swirling jet cases had more stabilized flames having the maximum temperature around 1560 K. The existence of internal recirculation zones (IRZ) played a major role in flow stabilization in swirling cases. Liang et al[38] employed TGA to investigate the co-combustion characteristics of wood, bamboo, moso bamboo, and masson pine. They observed volatile emission and oxidation combustion as two main combustion stages in the combustion process of samples. Torrefied biomass had only oxidation combustion stage in the combustion process. They found higher initial and burnout temperature for torrefied biomass in comparison to untreated biomass. They reported shift of combustion process towards higher temperature with increase in heating rate.

2.2.2 | Flow field, temperature distribution, and radiation effect

Ghenai and Janajreh[39] investigated the effect of biomass blending with coal on the distribution of velocity, gas, and particle temperature inside the combustor. They observed four recirculation zones in the furnace created by the four tabs placed in the furnace. They reported that these vortices helped in mixing coal and biomass particles efficiently which is the reason behind the increased combustion efficiency. Al-Widyan et al[40] utilized pulverized olive cake as alternative biomass and studied its combustion characteristics and emissions by varying equivalence ratio from 0.8 to 1.4. They obtained maximum combustion and thermal efficiency as 82% and 69%, respectively. They reported maximum flame temperature and cooling water temperature gradient as 980°C and 20°C. Smart et al[20] reported that biomass addition to coal has an adverse effect on radiative heat flux whereas burnout increases during co-firing. Bhuiyan and Naser[41] numerically studied oxy-fuel co-combustion characteristics of Russian coal and shea meal. They predicted the radiative and convective heat flux and presented the results through temperature distribution, CO_2 concentrations, etc. They investigated the effect of RR on the average, peak, and furnace exit temperature. They found optimum recycle ratio of 71% for flame temperature and radiative heat flux at 20% biomass sharing whereas optimum recycle ratio changed to 70% at 40% biomass sharing.

Bhuiyan and Naser[42] performed CFD analysis of co-combustion of coal with straw in the air and oxy-fired combustion conditions. They varied the combustion environment by changing oxidant concentration. They compared flame temperature under air fired and oxy-fired conditions for retrofitting purpose. Their results showing the effect of different fuel ratio on centerline temperature in air-fired and oxy-fired combustion conditions are shown in Figure 5. They obtained identical combustion characteristics to air-fired combustion environment at 30% oxygen concentration under oxy-fuel environment. They reported that up to 20% sharing of straw does not affect temperature profile significantly, whereas when sharing of straw was increased above 20%, flame temperature reduces. They further added that 100% straw firing raised the CO emission level as a consequence of an increase in residence time by increasing straw share in

ISSN NO: 9726-001X
Volume 10 Issue 03 2022

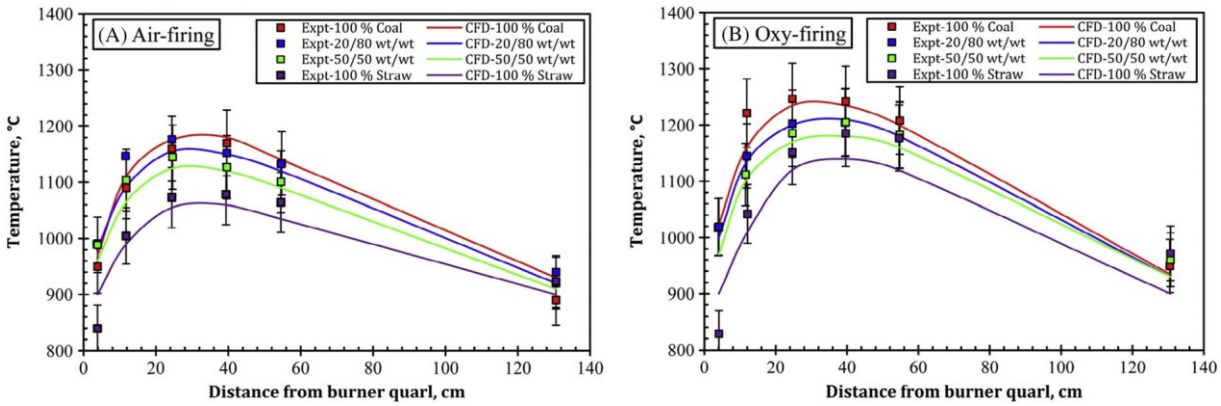

FIGURE 5 Influence of different fuel ratios on centerline temperature in (A) air and (B) oxy-fuel combustion conditions[42] [Colour figure can be viewed at wileyonlinelibrary.com]

fuel. Lv et al[43] performed the numerical investigation of co-combustion of coal and biomass in 600 MW boiler. They mainly focused on heat transfer and burnout characteristics under various operating conditions and for various biomass proportions. They reported decrease in average heat flux by switching from air to oxy-fuel conditions. The addition of biomass to coal had a positive influence on wall heat flux and wall heat flux increases with increase in biomass proportion.

2.2.3 | Environmental aspects of co-combustion

Gubba et al[44] investigated co-combustion characteristics of coal and wheat straw at two thermal loads in a tangentially fired 300 MW furnace. They reported a reduction in NO_x emission during co-firing. They further added that the 12% biomass share produced slightly less NO_x than the 6% biomass share. Ghenai and Janajreh[39] reported reduction in NO and CO_2 emission level during co-firing coal and biomass. Al-Widyan et al[40] reported the CO concentration around 1.6%, NO_x emission 550 ppm, and the maximum of SO_x level 30 ppm through the exhaust gas analysis during combustion of olive cake in the vertical furnace. Narayanan and Natarajan[45] performed co-combustion of bituminous coal with biomass (20%, 40%, and 60% mass proportions) to investigate the NO_x, SO_x, and suspended particulate matter (SPM) emission in an 18.68 MW power plant. They found reduction in NO_x and SO_2 emission by 45% and 50%, respectively, when co-fired wood with coal in 60% proportion of wood. They further added that SPM emission was also lowest for 40:60 proportion of coal:wood having a reduction of about 14% compared with 100% bituminous coal only firing. A quantitative summary showing the relationship between the biomass portion and reduction in NO_x and SO_x emission during co-firing is shown in Table 3. Kazagic and Smajevic[46] reported reduced NO_x and SO_2 emission at the reduced process temperature. They

TABLE 3 Quantitative summary showing the relationship between biomass portion and reduction in NO_x and SO_x emission during co-firing

Type of Biomass	Proportion of Biomass	Reduction in NO_x Emission (%)	Reduction in SO_x Emission (%)	Ref.
Wheat straw	6% and 12%	5% and 11%	_	Gubba et al[44]
Wheat straw	10% and 20%	23% and 42%	_	Ghenai and Janajreh[39]
Wood pellets	10%, 20%, 30%, and 100%	18%, 26%, 32%, and 90%	13%, 19%, 25%, and 100%	Moroń and Rybak[119]
Wood	20%, 40%, and 60%	18%, 36%, and 45%	16%, 37%, and 50%	Narayanan and Natarajan[45]
Torrefied spruce	50%	36%	44%	Ndibe et al[55]
Refuse derived fuel (RDF)	50%	43%	58%	Chen et al[143]
White pine pellets	20%, 50%, 80%, and 100%	18%, 42%, 58%, and 72%	13%, 29%, 44%, and 52%	Badour et al[144]
Wood chips	20% and 60%	13% and 41%	17% and 56%	Nussbaumer[145]
Straw	20%, 40%, 60%, and 100%	15%, 22%, 44%, and 55%	_	Wang et al[146]
Olive waste	10% and 20%	13% and 25%	_	Riaza et al[19]

JOURNAL OF CURRENT SCIENCE

obtained 50% reduction in NO_x by reducing process temperature from 1400°C to 960°C. Gil et al[47] reported low NO emission by addition of biomass. Steer et al[48] also reported reduced NO_x and increased CO emission during co-firing in a 500 MW down-fired boiler.

Particulate matter emission has a strong dependency on the biomass to coal blending ratio, type, and composition of coal. Regarding particle matter emission different authors have different opinion. Some authors[49-52] reported that emission of particulate matter increases during co-firing coal with biomass due to the higher amount of alkali metal and chlorine in biomass, whereas others[45,53,54] reported reduced particulate matter emission during co-firing.

Nzihou and Stanmore[51] explored the effects of co-combustion on ultrafine aerosol particle formation. They reported that biomass has greater alkali metal content and coal is higher in ash and sulfur content, which is responsible for increased ultra-fine aerosol particle formation during co-firing. Ultra-fine aerosol particles are known to produce adverse pulmonary effects. Wu et al[49] also reported increased formation of the submicron particle, especially ultrafine particles below 0.2 μm during co-combustion of bituminous coal and solid recovered fuel (SRF). Ndibe et al[55] investigated co-combustion behavior of torrefied biomass in a drop tube furnace (DTF) at 50% thermal shares with coal. They evaluated combustion reactivity, burnout, and emission characteristics of torrefied biomass, non-thermally treated wood pellets, a highly volatile bituminous coal and lignite coal. They reported reduced SO_2 emission due to dilution when woody biomass is blended with coal, whereas NO_x emission depends on factors such as volatile matter in fuel, type of fuel, burner, and furnace configurations. In air staged co-firing nitrogen converted to NO_x decreased from 34% to 9% than unstaged combustion. In mono combustion cases, nitrogen converted to NO_x also reduced from 42% to 10%.

Vekemans et al[56] injected $CaCO_3$ and $Ca(OH)_2$ with coal and reported reduced sulfur emission by 18% and 20% with $Ca(OH)_2$ and $CaCO_3$, respectively. They further added that co-firing of waste-derived fuel ReEF™ at 20% thermal share reduced SO_2 emission by 20%. Co-firing of ReEF™ emitted HCl more than 20 ppm as ReEF™ contains PVC.

2.3 | Ash formation and deposition

Pulverized coal after complex physical and chemical transformations during combustion produces ash which can be in the form of liquid, vapor, and solid. The composition of coal and combustion conditions affects the composition and size of intermediate ash species. Fouling, slagging, erosion, and corrosion problems are strongly influenced by the composition and size of intermediate ash species. Fouling deposits are friable ash which adheres to the heat transfer tubes in the convection zone and increases heat transfer resistance in the convection zone. Slagging deposits are produced from fused ash which sticks on the walls of the furnace and changes the radiative heat transfer in the radiation zone. Fine ash is the particulate matter that is the primary cause of air pollution. Therefore, understanding of ash formation and deposition is required during coal combustion.

Niu et al[57] presented the in-depth review of major problems associated with ash formation and deposition such as alkali-induced slagging, silicate melt-induced slagging (ash fusion), and agglomeration. They also suggested the solution of above ash-related problems by the use of additives, co-firing, and leaching. They also discussed the corrosion problem of ash by the use of different corrosion mechanisms. Alkali chlorides and sulfates play a vital role in alkali-induced slagging, and its chemistry is strongly dependent on ash compositions (such as alkalis concentrations, Cl, S, Al, Si etc.), combustion conditions, and combustion temperature. Silicate melt-induced slagging (ash fusion) is dependent on both elemental compositions and mineral compositions. Agglomeration usually occurs in the fluidized bed due to interactions of ash-forming elements and bed particles. Agglomeration process is strongly influenced by the bed material. Gaseous or liquid K compounds react to bed particles and initiate the agglomeration process. Kurose et al[58] examined how combustion characteristics of pulverized coal are influenced by ash content in coal in both staged and standard combustion conditions. For their work, they tested three different coals having 36, 44, and 55 wt% of ash contents. They reported a reduction in gas temperature and increase in unburnt carbon (UBC) at furnace exit by an increase in the ash content. They further added that staged combustion produced more UBC at furnace exit than the standard combustion. Kazagic and Smajevic[46] analyzed the ash behavior of co-fired Bosnian coal and biomass. They observed very low ash deposits at 1100°C, but ash deposition becomes moderate with soft deposits when the temperature was raised to 1300°C. They further added that at the temperature above 1300°C, severe fouling and slagging which are hard to remove are formed for all type of coal. They got similar trends when compared these results with measurement in the real boilers. Measurement and mathematical modeling of fly ash deposition were done

ISSN NO: 9726-001X
Volume 10 Issue 03 2022

by Beckmann et al[59] in a 15-kW jet flame. They reported that deposition rates had been increased using the air-cooled probe in comparison to uncooled probe. They further added that the deposition rate is strongly dependent on the probe location and the probe surface temperature. Jayanti et al[60] employed CFD modeling to study how char reactivity, the diffusion rate of oxygen for char combustion, and radiation heat transfer got affected by ash content in coal and found that increased ash content had negligible effect on enhanced char reactivity whereas thicker ash layer caused reduced char oxidation rate resulting from reduced diffusion rate of oxygen. They reported a reduction in thermal load by 33% for the maximum ash content of 40%, which causes the reduction in peak temperature by about 100 K compared with the reference case (10.8% ash). Their results were consistent with the experimental observation of Kurose et al.[58] When they maintained overall thermal load constant by the increasing coal flow rate for the compensation of reduction in calorific value as the ash content was increased, they observed both peak temperature and flue gas temperature were insignificant to increase in ash content. Laxminarayan et al[61] investigated the deposit formation of a model biomass ash species ($K_2Si_4O_9$) on steel tubes in entrained flow reactor (EFR). They injected $K_2Si_4O_9$ into the reactor, which formed deposits on an air-cooled probe. They investigated the effect of surface temperature of probe, temperature and velocity of flue gas, probe residence time, and fly ash flux. They reported that the sticking probability of the fly ash particles increases with increasing probe surface temperature and flue gas temperature, which increases the deposition rate. Increase in flue gas velocity reduces deposit formation rate due to increased rebound. Furthermore, they found an increased deposition rate with probe residence time and fly ash flux.

2.4 | Heat transfer in pulverized coal furnaces

Accurate prediction of heat transfer is required for modeling combustion in pulverized fired furnaces. Radiation is the dominant mode of heat transfer due to the extremely high temperature produced in the pulverized fired furnaces in the air as well as oxy-fuel combustion environment. Viskanta and Menguc[62] proposed the radiative transfer equation (RTE) in the direction of a pencil of rays within a certain elemental solid angle. Radiation heat transfer within the furnace is predicted by solving the RTE and coupling it with models of radiative properties.

$$\frac{dI_\lambda(\vec{r},\vec{s})}{ds} = -(k_{a,\lambda}+\sigma_{s,\lambda})I_\lambda(\vec{r},\vec{s}) + k_{a,\lambda}I_{\lambda,b} + \frac{\sigma_{s,\lambda}}{4\pi}\int_{\Omega=0}^{4\pi} I_\lambda(\vec{r},\vec{s}')\Phi(\vec{s},\vec{s}')\,d\Omega' \quad (1)$$

The RTE is solved by the solvers which include spherical harmonics (P1) method, discrete ordinates (DO) method, Monte Carlo method (MCM), and discrete transfer ray tracing method (DTRM). Each method has its benefits and limitations. P1 model is employed for the medium having large optical dimension. The DO model is more accurate and suitable for all optic thickness but computationally expansive. Whereas the DTRM model has less accuracy than DO model but appropriate for the large range of optic thickness. The selection of the method depends on the type of problem.[4]

Cai et al[63] developed a Favre averaging method for reacting multiphase turbulent flows, in which both continuous and dispersed phases were modeled in the Eulerian frame of reference. Along with Favre averaging, a new nongray radiation model was used. They observed solid phase temperature was affected more by the size than velocity. They reported 500 K decrease in temperature of solid phases by radiation cooling. They observed radiation's indirect effect on CO_2 prediction through heavily temperature-dependent char reaction rates. They further added that both CO_2 and temperature predictions improved by considering radiation. Hashimoto and Watanabe[64] studied how heat transfer mechanism is affected by furnace scale and investigated heat transfer mechanism in 915 MW large boiler 2.4 MW and 0.76 MW test furnaces. They reported that small-scale furnace has shorter residence time due to the higher temperature of the particles than the large-scale furnace. They further added that particles of the small-scale furnace have an inadequate heat gain as thinner flames have less radiative heat transfer. Yu et al[65] proposed a model for pulverized coal particles which takes heat and mass transfers in the boundary layer region and chemical reactions into account. They reported that the volatiles of coal particles ignited at 4.8 ms and pyrolysis rate reaches a maximum at 13.8 ms. They found that ignition of CO could occur in the boundary layer of the particle in actual pulverized coal flame due to the ignition effect of the volatile flame. Kumar and Sahu[66] modeled 210 MW boiler using CFD to study the effect of burner tilt angle on the mechanism of coal combustion, distribution of heat flux, and furnace exit gas temperature (FEGT). They reported that changing burner tilt angle affected the distribution of heat flux within the furnace and temperature profile significantly. They further added that variation of tilt angle from −30° to +15° reduced the distribution of the heat flux to the bottom ash hopper by 70 MW and

increased distributed heat flux to the center and top portions by 5 and 22 MW, respectively. Jayanti et al[60] investigated the effect of ash content on radiative heat transfer parameters numerically using CFD code. They reported transferred heat through the walls and outlet of the furnace as 2.364 and 1.597 MW. Crnomarkovic et al[67] investigated the effect of the scattering albedo and total extinction coefficient on radiation heat transfer through the furnace wall employing Hottel's zonal model. They reported the maximum heat transfer rate and wall flux at moderate values of extinction coefficient. They found that heat transfer rate and wall flux values were higher for smaller extinction coefficient than for larger extinction coefficient. They further added that both heat transfer rate and wall flux reduced with the increase in scattering albedo. Chakraborty et al[68] developed a numerical model for pusher type reheating furnace to insight into the parameters playing a vital role in the complex combustion processes. They found the dominance of radiation heat transfer over convection heat transfer. They reported the efficiency of reheating furnaces as 51%. They observed periodic heating characteristics of billet from the entrance to discharge door. Zhang et al[69] proposed a flue gas temperature estimation approach in the boiler by a dynamic heat transfer model. They also calculated the proportion of convective heat for semi radiative heat exchanger. They found their model very feasible as it gives flue gas temperature very close to designed value. They reported the average relative error of estimated flue gas temperature at the final reheater outlet to be 1.4% in the 24 hours.

2.5 | Numerical analysis of pulverized coal combustion process

CFD modeling has emerged as a powerful and unexpansive tool for design and development of pulverized coal-fired furnaces. Complex physical and chemical processes of the pulverized coal combustion can be dealt accurately through detailed simulation tools and suitable submodels. Numerical modeling employing CFD tools saves manpower and time and also shortens maintenance period in the large-scale boilers. Therefore, CFD modeling of combustion processes is supposed to play an essential role in the development of combustion systems in the future.

The combustion process of pulverized coal is typically modeled as dilute two-phase reacting flow employing the Eulerian-Lagrangian approach. The submodels of gas phase have the description of fluid flow, heat and mass transfer, and chemical reactions.[7]

In the CFD simulations, gas phase is most commonly modeled employing RANS and LES approach. The RANS-based approach decomposes the dependent variable into space-time averaged components and fluctuations. Transport equations for turbulent properties such as turbulent viscosity, turbulent kinetic energy, and turbulent dissipation rate are solved to model the resulting Reynolds fluxes. In LES, large eddies are resolved directly whereas the impact of the smaller eddies are modelled.[2]

Most commonly used turbulence model is a k-ε model, having three variants (Standard, RNG, and Realizable). The standard k-ε model assumes flow as fully turbulent and neglects the effect of molecular viscosity. Thus, it is valid only for fully turbulent flows. The standard k-ε model is modified into RNG and realizable k-ε model to overcome its limitation. In RNG, k-ε model effect of swirl on turbulence is included which enhances its prediction accuracy of swirling flows. This model also has an additional term in the ε equation that improves the accuracy of rapidly strained flows. These features of RNG k-ε make it more reliable and accurate than the standard k-ε model for the wider class of flows. In the realizable k-ε model, turbulent viscosity is formulated alternatively, and modified transport equation for dissipation rate "ε" has been derived from the exact solution of the transport of mean square vorticity fluctuation. The realizable k-ε model meets certain mathematical constraints on Reynolds stresses that correspond to the physics of turbulent flows. The flows involving rotation, recirculation, and boundary layers under strong adverse pressure gradients can be accurately predicted by realizable k-ε model.[70]

Figure 6 shows the systematic approach of pulverized coal-fired combustion modeling. Summary of numerical work along with various modeling approaches is given in Table 4.

Sadiki et al[71] numerically studied the combustion behavior of pulverized coal in the oxy-fuel combustion environment and compared combustion properties predicted by LES and RANS along with associated multiphase phenomenon. For the above purpose, they developed the Eulerian-Lagrangian approach-based oxy-fuel combustion module. The developed model consisted of turbulence models, models for coal particle transport, models for radiation heat transfer, models for devolatilization, and homogeneous and heterogeneous combustion models. They reported satisfactory agreement for both LES and RANS predictions whereas their prediction capability differs by some extents. Continuous gas phase and dispersed particle phase interactions were taken care of by two-way coupling. They found that LES modeling coupled with turbulent dispersion model has better predictability than RANS, and the

ISSN NO: 9726-001X
Volume 10 Issue 03 2022

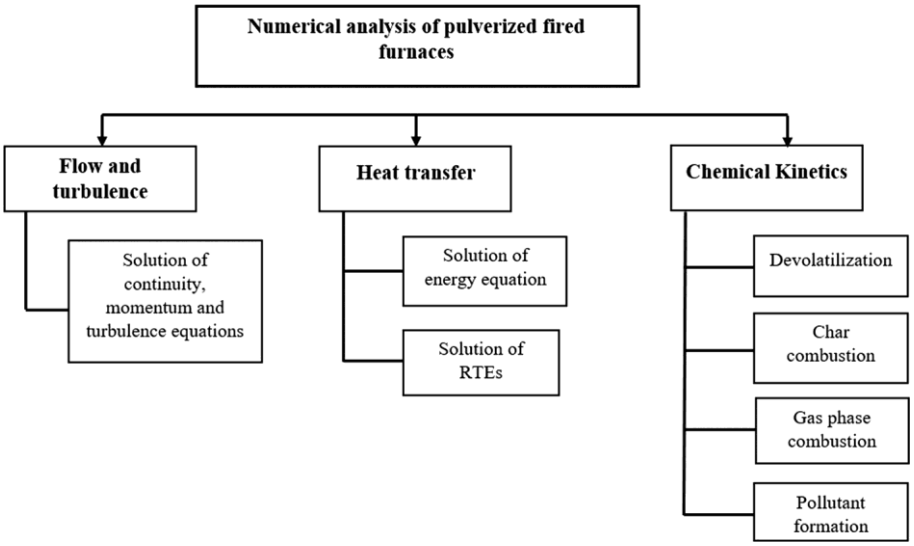

FIGURE 6 CFD modeling of pulverized coal combustion: An overview of basic modules[73]

combustion properties were significantly affected by the devolatilization kinetics, due to which turbulence intensity was modified throughout the combustion chamber. Kangwanpongpan et al[72] employed DO method coupled with the weighted sum gray gas model to predict the radiative properties in oxy-fuel combustion conditions. They observed difference between measured and predicted velocity and oxygen concentration near the burner due to the inaccurate thermochemical closure and limitations of the turbulence model. They reported that the optimized parameters better predicted the gas flame temperatures under oxy-fired conditions, which was noticeably lower than the value predicted under the air-fired condition. Similar trends were observed for radiation heat transfer at the lateral wall.

Wu et al[74] studied the combustion and ignition properties of bituminous coal (Datong) under oxy-fired and air-fired combustion environment by employing an unsteady state model for pulverized coal cloud including various submodels of convection and radiation. They also investigated ignition temperature of bituminous coal by replacing air with the mixture of oxygen and RFG. They reported that the pulverized coal ignition was delayed under oxy-fuel combustion because of the CO_2's different property compared with N_2. They observed that ignition temperature was increased by 10 to 50 K when the atmosphere changes from air to oxy-fuel with similar oxygen content. Figure 7 shows the numerical simulation results of Warzecha and Boguslawski[75] in the process of pulverized coal combustion employing Reynolds-averaged Navier-Stokes (RANS equations) and large eddy simulation (LES) methods in swirl burner for turbulent flow. They observed the notable variation of temperature at burner exit while comparing the combustion process in the air and oxy-fuel environment. They validated their numerical data with measured and simulated data of other authors. They obtained a strong inner recirculation zone for both RANS and LES models, but LES produced more accurate results. They observed outer recirculation zone for LES. They reported the considerable reduction in temperature and velocity distribution in the combustion chamber by changing the combustion environment from air to oxy-fuel.

Gaikwad et al[76] performed 2D CFD simulation of the test facility of Institute of Heat and Mass Transfer of RWTH Aachen University to analyze combustion behavior of pulverized coal in the oxy-fuel environment employing swirl burner. They evaluated the performance of radiation and turbulent models to study the pulverized coal combustion processes and reported that the Do radiation model with domain-based WSGGM and SST k-ω turbulence model showed a good agreement with measured data among other tested models. Franchetti et al[77] performed LES simulation of the pulverized coal combustion process and addressed its merits and demerits by comparing results with measured data of flow field, temperature, and species concentration. They employed Eulerian and Lagrangian approach for gas and particle phase, respectively. They reported that LES slightly overpredicted average particle velocity at z = 60 mm and a slightly underpredicted at z = 120 mm, at other location prediction of LES match with experimental results. They observed that oxygen consumption rate was overpredicted by the EBU model. Thus, they recommended finite chemistry models for volatile combustion. Ahn et al[78] performed LES of the co-axial jet flame of pulverized coal employing SGS (Smagorinsky) model and Lagrangian tracking of particles. They validated numerical results with measured data and observed narrow particle dispersion in combustion cases than

TABLE 4 Summary of numerical work along with employed models and submodels of combustion

			Modeling Approaches				
Facility	Fuel	Code	Turbulence	Radiation	Devolatilization	Char Combustion	Ref.
RWTH Aachen 100 kW down fired swirl burner furnace	Lignite coal	Fluent 15.0	Standard k-ε RNG k-ε SST k-ω	DO	Single kinetic rate model	Kinetics/diffusion-limited	Gaikwad et al[76]
35 MW large pilot boiler	Sub-bituminous	Fluent 16.0	Realizable k-ε	WSGGM	CPD	Kinetics/diffusion-limited	Guo et al[26]
Downward fired cylindrical chamber of capacity 60 kW	Lignite coal	Fluent 17.0	Realizable k-ε	P1	Single kinetic rate model	Kinetics/diffusion-limited	Sadiki et al[71]
600 MW pulverized-coalutility boiler	Pulverized coal	Fluent	Realizable k-ε	DO	Two competing rate model	Kinetics/diffusion-limited	Ti et al[147]
915 MW actual large-scale boiler, 2.4 MW and 0.76 MW test furnaces	Pulverized coal	Fluent	RNG K-ε	DO	Modified TDP model	Combined model of kinetics andeddy dissipation	Hashimoto et al[64]
15 kW test furnace	Bituminous coal	Fluent	Standard k-ε	_	Two competing rate model (Kobayashi model)	Intrinsic charburnout model	Beckmann et al[59]
300 MW tangentially fired pulverized coal furnace	Pulverized coal	Fluent	Standard k-ε RNG K-ε RSM	DO	Single kinetic rate model	Diffusion-limited	Khaldi et al[148]
0.3 MW pilot-scale furnace	Pulverized coal	Fluent	Standard k-ε	P1	CPD	_	Tu et al[149]
200 MW tangentially fired utility boiler	Bituminous coal	Fluent 6.3	Standard k-ε	Improved WSGG model	CPD	Kinetics/diffusion-limited	Guo et al[150]
Drop tube furnace	Bituminous coal	Fluent 12.0	Standard k-ε	DO	Single kinetic rate model	Kinetics/diffusion-limited	Cai et al[63]
RWEn power's 0.5MWth combustion test facility (CTF)	Pulverized coal	Fluent	Standard k-ε	DO	CPD	_	Rebola and Azevedo[27]
2.5 MW pilot combustion test facility	Gottelborn coal	Fluent	Standard k-ε	DO	CPD	_	Rebola and Azevedo[151]
_	Pulverized coal	MFIX	Standard k-ε	P1	Kobayashi's model Ubhayakar's model	A half-order reaction rate of Harmor	Cai et al[152]
RWTH Aachen 100 kW down fired swirl burner furnace	Lignite coal	Fluent	Standard k-ε	DO	Single kinetic rate model	_	Warzecha and Boguslawski[75]
CRIEPI's coaxial jet burner	Pulverized coal	_	SGS turbulent model (LES)	_	FLASHCHAIN	Global 2 step kinetic mechanism	Ahn et al[78]

(Continues)

ISSN NO: 9726-001X
Volume 10 Issue 03 2022

TABLE 4 (Continued)

Facility	Fuel	Modeling Approaches					Ref.
		Code	Turbulence	Radiation	Devolatilization	Char Combustion	
Pusher type reheating furnace	Pulverized coal	Fluent 15.0	Realizable K-ε	WSGGM	Two competing rate model	Intrinsic kinetic rate model	Chakraborty et al[68]
600 MW wall-fired boiler	Pulverized coal	Fluent	Standard k-ε	P1	Two competing rate model	Kinetics/diffusion-limited	Du et al[153]
Vertical cylindrical laboratory furnace	Coal/biomass (80:20)	Fluent 6.3	_	DO	Two competing rate model	Kinetics/diffusion-limited	Bonefacic et al[79]

non-combustion case by means of axial interphase momentum transfer. They reported early breakdown of cylindrical shaped particles in combustion case due to the devolatilized gas combustion. They obtained good agreement between numerical results and measured data. Bonefacic et al[79] performed numerical simulation of co-combustion of pulverized coal and biomass in a cylindrical laboratory furnace by mixing 20% biomass with coal. They modeled various physical and chemical processes such as turbulent flow, heat and mass transfer, devolatilization, and char combustion. They reported that the developed model described the shape of biomass particles as cylinders whereas existing models describe particles as spheres. They further added that the developed model more accurately predicted the concentrations of carbon monoxide and nitrogen monoxide in the flue gas than existing models. They observed that devolatilization rate and coke residue burning was affected by the geometry significantly. Purimetla and Cui[80] studied burner secondary airflow balancing by CFD modeling of fossil power plant wind box by solving 3D RANS equations. They validated their results with measured data obtained from a 1/8th scale model of the furnace. They reported that the position of the third baffle diminishes the uniform distribution of secondary flow, and, therefore, it cannot be suitable in practice. Madejski[81] presented the results of a numerical simulation of front wall fired pulverized coal boiler. He developed models for various key combustion processes such as heating, devolatilization, char combustion, turbulence, and radiation. The results showed the proper location of over fire air (OFA) nozzle.

2.6 | Thermodynamic analysis of coal combustion

Thermodynamic analysis of the combustion processes done by flow availability to the system comprising the entire combustor.

$$A_{in} \frac{1}{4} A_e \text{ þ } I \quad (2)$$

where A_{in} and A_e are the incoming and outgoing flow availability rates of the system, and I is the thermodynamic irreversibility rate within the system.

Som et al[82] evaluated second law efficiency and thermodynamic irreversibility in the process of pulverized coal combustion in the tubular combustor. They employed the Eulerian-Lagrangian frame of reference-based two-phase separated flow model to compute velocity, temperature, and species concentration. They determined the total thermodynamic irreversibility by taking the difference of flow availabilities at inlet and outlet.

ISSN NO: 9726-001X
Volume 10 Issue 03 2022

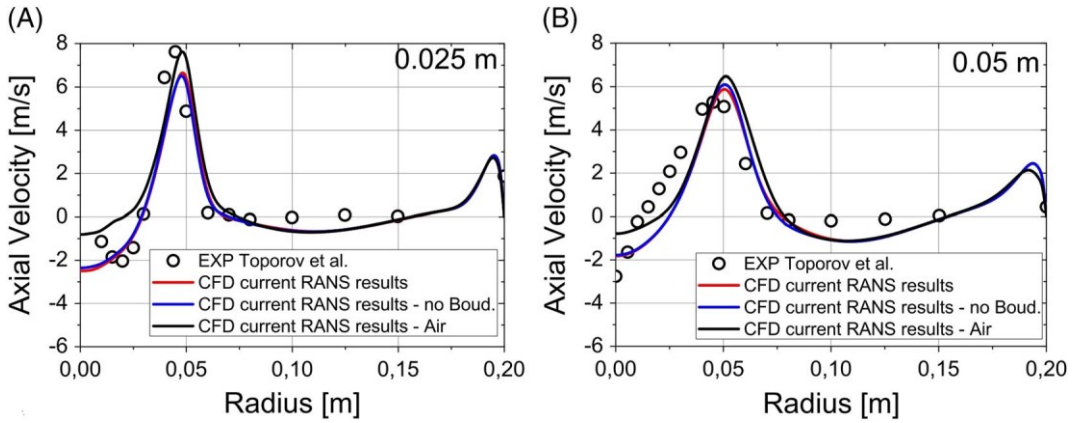

FIGURE 7 Comparison of axial velocity prediction at axial locations (A) 0.025 m and (B) 0.05 m employing RANS and LES[75] [Colour figure can be viewed at wileyonlinelibrary.com]

They reported that the increase in inlet air pressure leads to an increase in combustion efficiency and a decrease in second law efficiency. They found these influences more effective at low swirl number and in shorter combustor length. They obtained the increase in combustion efficiency when swirl number was increased from S = 0.0 to 0.32, whereas the further increase in swirl number from 0.32 to 0.77 resulted in reduced combustion efficiency. They reported reduced combustion efficiency with increasing air temperature for the smaller length of the combustor and increased combustion efficiency for a longer length of the combustor.

Mondal[83] presented a mathematical model for various physical processes involved and associated thermodynamic irreversibility in the combustion process of pulverized coal in the quiescent hot medium. The homogeneous and heterogeneous chemical reactions in the particle and gas phase were considered by solving continuity, momentum, and energy conservation equation in the spherical coordinate. Generalized entropy conservation equation was used to estimate the thermodynamic irreversibility due to gas-phase chemical reactions and various transport processes. He explained the cause of thermodynamic irreversibility as the combined effect of heat transfer as well as mass transfer in the gas phase and chemical reactions. Additionally, he concluded that initially irreversibility rate was low but increased rapidly as ignition proceeds then finally decreased to the steady-state value as shown in Figure 8. Som and Sharma[84] evaluated second law efficiency and thermodynamic irreversibility in the process of spray combustion in the gas turbine combustor for different volatile fuels. The flow availability and process irreversibility have been calculated from the computed values of velocity, temperature, and species concentration. The total thermodynamic irreversibility was determined by the difference of inlet and outlet flow availability. They reported increased combustion efficiency with increase in fuel volatility at high pressure for given swirl and inlet temperature. They observed that combustion efficiency was uninfluenced by the inlet swirl at lower pressure whereas at higher pressure both second law efficiency and combustion efficiency decrease with increasing the value of inlet

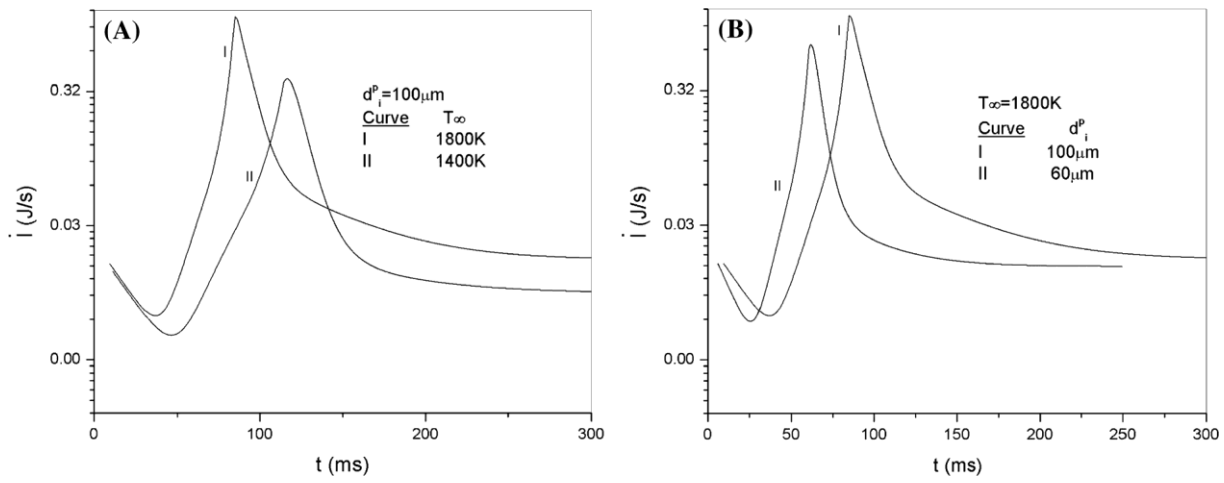

FIGURE 8 Temporal histories of irreversibility rate for different values of (A) free stream temperature and (B) initial particle diameter[83]

swirl. They further added that second law efficiency increases by the reduction of fuel volatility and an increase in combustor pressure. Spray cone angle also affects second law efficiency and combustion efficiency, and both the parameters increase with increase in spray cone angle. Som and Datta[85] presented a detailed review on exergy loss and thermodynamic irreversibility in the combustion process of solid, liquid, and gaseous fuel. They reported chemical reactions and physical transport processes as the source of irreversibility in the combustion process. They further added that exergy destruction rate due to chemical reactions could be decreased by the rise in flame temperature. They emphasized the development of combustion systems which were energy and exergy efficient. They further added that there is a need for better understanding of how vorticity and turbulence affect entropy production in various flames. Xiong et al[86] carried out exergy analysis of 600 MW pulverized coal-fired oxy-fuel combustion process. They also compared the results of two different boiler models for exergy analysis. They reported furnace exergy efficiency of oxy-fuel combustion was 4% more than that of the conventional combustion system. They further added that highest exergy destruction (about 60%) was due to the combustion process. They observed low exergy penalty in oxy-fired combustion boiler than that of the air-fired. Wang et al[87] developed a novel hydrogen-fueled power plant for CO_2 capture based on calcium looping process and evaluated exergy loss due to various processes during the combustion. They reported exergy and energy efficiency of the system as 42.25% and 42.7%, respectively. They further added that combustion chamber and regenerator were the primary sources of exergy destruction as a result of associated irreversibilities of the chemical reactions. They showed that increases in gas turbine inlet temperature and air pressure ratio lead to higher thermal efficiency. Wang et al[88] numerically investigated the unsteady entropy generation, heat, and chemical species transfer in transient oxy-combustion of single coal. The result showed that the production and transport rates of species reached maximum level in the process of homogeneous combustion of volatiles. They reported chemical reaction as the most significant source of unsteady irreversibility. They found increased total chemical entropy generation due to oxygenation of the atmosphere. The increase of total chemical entropy generation becomes almost insensitive after certain oxygen mole fraction.

2.7 | Devolatilization models

During the devolatilization process, tar and light gases are released from the coal in an endothermic process. Stability of flames, temperature profile, and emissions are strongly dependent on the devolatilization process. The devolatilization models determine the rate at which volatile matter is released from coal. The following well-known devolatilization models are used to study the devolatilization process.

The release of volatiles takes place at a constant rate in the constant rate model developed by Baum and Street.[89] Approximate value of vaporization temperature is assigned to the constant rate model. Constant rate devolatilization model could not predict accurately that is why this model is only used for initialization of flame at the beginning of the simulation.

Volatile release rate shows first-order dependency on the peak combustion temperature and quantity of released volatile matter in the single kinetic rate model developed by Badzioch and Hawksley.[90] For accurate prediction using single kinetic rate model, the volatile fraction in coal should be considered more than the determined value of proximate analysis as proximate analysis is performed at the lower temperature than the actual combustion temperature. Coal-dependent rate parameters are the limitation of this model.

In the two-competing rate model,[91,92] devolatilization rate shows dependency on two coupling rates over the different temperature range. The volatile fraction prediction is influenced by the heating rate of multiple steps. Again, dependency on coal type is the limitation of this model.

Chemical structure-based network models are the most detailed approach to simulate the decomposition. Network models do not show dependency on coal proximate analysis data. Hence, they can accurately predict volatile release rate in the coal combustion process. Network-based devolatilization models are based on parent coal's chemical structure which is simplified as a chemical bridge lattice. Flash distillation analogy-based network model was suggested by Niksa[93] which was developed further. Parent coal's chemical structure based Chemical Percolation-Devolatilization (CPD) model was developed and modified by Fletcher et al[94,95] and Grant et al.[96] The devolatilization behavior of heated coal particle is characterized by both chemical and physical transformation of coal structure in CPD model.

Smoot and Smith,[97] Solomon and Fletcher[98] developed network pyrolysis dependent Functional Group-Depolymerization Vaporization Cross-linking (FG-DVC) devolatilization model. A two-stage pre-processed program predicts the gas, tar, and char yields in the process of combustion from the initial analysis of parent coal.

Goshayeshi and Sutherland[99] evaluated the effectiveness of gas-phase chemistry models (detailed kinetics and a flame-sheet model) and devolatilization models (CPD and the Kobayashi-Sarofim model) for combustion

of pulverized coal particles. They reported that the CPD model coupled with the detailed gas-phase chemistry gives good agreement to experimental observations whereas Kobayashi-Sarofim model coupled with the flame-sheet model only captured trends of experimental measurements. They further added that modeling of devolatilization process and gas phase chemistry is necessary for the understanding of the ignition behavior. Kumar and Sahu[66] reported variation in residence time of coal particle by varying burner tilt angle. They reported that the devolatilization of particles of 50 to 120-µm size completes within 60 to 80 ms, whereas char oxidation time is a strong function of particle size and varies at the exponential rate with particle size. Zou et al[100] investigated the homogeneous and heterogeneous processes and the effects of particle size and ambient gas temperature on the ignition mechanism of the pulverized coal particles in the O_2/CO_2 combustion environment. They adopted the single rate kinetic model for devolatilization. They reported homogeneous ignition for coal particles of 85-µm diameter in secondary air temperature from 1073 to 1473 K in O_2/CO_2 atmospheres having 0.21 mole fraction of O_2. They further added that as the O_2 mole fraction in the O_2/CO_2 atmosphere was increased, the secondary air temperature range at which homogeneous ignition occurs decreases. They observed secondary air temperature range of 1073 to 1273 K at an oxygen mole fraction of 0.35 in the O_2/CO_2 atmosphere. They found homogeneous ignition for large particles and heterogeneous ignition for small coal particles. Cai et al[63] investigated the ignition behavior of coal particles in O_2/N_2 and O_2/H_2O environment by varying oxygen concentration from 21% to 50% in DTF employing a high-speed camera. They observed homogeneous ignition in both O_2/N_2 and O_2/H_2O combustion environment but earlier ignition in the O_2/H_2O atmosphere than O_2/N_2 at similar oxygen mole fraction due to the steam shift reaction in the O_2/H_2O atmosphere. Richards and Fletcher[101] compared seven simple devolatilization models with well-known CPD model and found that the modified two-step model with distributed activation energy yielded close predictions with that of CPD while the simple single step model predictions were not comparable.

2.8 | Single coal particle combustion

Under this section, attempts have been made to review single coal particle combustion.

Zhou et al[22] employed continuous-film model to address the overall and separate effects of carbon dioxide on the combustion of bituminous Pittsburgh coal char in both air and oxy-fuel combustion conditions. They analyzed various effects of carbon dioxide (CO_2) on the particle temperature and rate of combustion in the oxy-fuel environment. They explored the influence of oxygen concentration, chemical, and thermal effects on coal char combustion to explain the mechanism in oxy-fuel combustion. They reported the contribution of oxygen concentration, thermal, and chemical effects as 6.7%, 11.2%, and 82.1% on char combustion rate of 91-µm char at an ambient gas temperature of 1200 K. Lee and Choi[102] visualized the burning of a single coal particle in the entrained hot gas flow. They showed the combustion process sequence in space and time by processes of particle heat-up, the release of volatile matter and its oxidation, and char combustion. They reported that the oxygen concentration strongly affected the appearance of the volatile flames. They observed volatile flames as spherically concentric in the enriched oxygen having the negligible effect of the particle's relative speed to the mean gas flow. Khatami et al[103] investigated the ignition behavior of a single coal particle in the air fired and oxy-fired conditions by varying oxygen mole fraction from 20% to 100%. They employed a bituminous, a sub-bituminous, and two lignite coals and char of these coals in the investigation. They reported homogeneous ignition for bituminous coal and heterogeneous ignition for lignite coal in both O_2/N_2 and O_2/CO_2 atmosphere. They observed the higher value of ignition delay in oxy-fuel combustion conditions and reduction in ignition delay when the oxygen concentration is increased in both oxy-fuel and air combustion condition. Combustion behavior of single bituminous and lignite coal particle and spherical and monodisperse synthetic char were investigated by Bejarano and Levendis[104] in both O_2/CO_2 and O_2/N_2 atmosphere. They reported increased coal particle temperature by increasing O_2 mole fraction in both the environments. They obtained the reduction of 250 and 200 K in flame temperature and char surface temperature by changing the combustion environment from air to oxy-fuel at identical oxygen mole fraction. This drop was smaller for lignite coal. Mondal[83] discussed the thermodynamic irreversibilities due to chemical reaction and transport processes in the process of single particle combustion. He determined the thermodynamic irreversibility contributed by chemical reaction and transport processes by generalized entropy conservation equation. He explained the cause of thermodynamic irreversibility as coupling effect of heat and mass transfer in the gas phase and chemical reactions. Zhou et al[105] investigated the ignition and combustion characteristics of single coal and biomass particles under O_2/N_2 and O_2/H_2O combustion atmosphere. They recorded ignition and combustion processes by CCD camera. They employed two-color pyrometry for volatile flame temperature and char combustion temperature measurement.

They found heterogeneous ignition of coal in both O_2/N_2 and O_2/H_2O combustion atmosphere at O_2 content of 21% to 50% whereas biomass ignites homogeneously when the oxidizer had O_2 content of 21% to 30% and heterogeneously for O_2 content of 40% to 50% in O_2/N_2 combustion atmosphere. In O_2/H_2O, homogeneous ignition of biomass occurs for O_2 content of 21% to 50%.

2.9 | Char combustion modeling

Combustion of coal char is the most important step in the process of pulverized coal combustion, and it affects both heat transfer in furnace and efficiency of the combustion process by influencing the residence time. Coal char combustion shows dependency on the structure and composition of coal along with the operating pressure, temperature, and oxygen concentration. The temperature of coal char is dependent on the mechanism of heat and mass transfer, heat flux distribution, and burning rate. Thus, for accurate calculation of char particle temperature, correct prediction of burning rate is essential.

Hecht et al[106] developed the Surface Kinetics in Porous particles (SKIPPY) for different sizes of pulverized coal char at the University of Sydney. Surface Kinetics in Porous particles (SKIPPY) is a FORTRAN-based computer program to solve conservation equations of mass, energy and species in which multicomponent diffusion and mass convection are taken care. Surface Kinetics in Porous particles (SKIPPY) accurately predicts temperature and species concentration within the boundary layer surrounding the char, at the outer surface of the char, and within the char pores. Kinetics in Porous particles (SKIPPY) predicted the effect of CO_2 gasification reaction on the consumption of pulverized coal char in the oxy-fuel atmosphere and reported that the balance of CO and CO_2 with reacting char particle is influenced by the CO_2 gasification reaction. They observed that both the char temperature and char oxidation rate drop significantly due to endothermicity of CO_2 gasification reaction. Hecht et al[107] extended their previous work and investigated the effect of steam gasification reaction along with CO_2 gasification reaction on pulverized coal char in the oxy-fuel combustion environment. They computed the characteristics of char consumption for 100-µm char particle in varying concentrations of O_2, CO_2, and H_2O employing SKIPPY model. They found that char particle temperature reduced significantly, and this decrease in char particle temperature leads to the decrease of char oxidation rate and radiant emission from burning char particle. They reported that carbon consumption rate is increased by 10% due to the combined effect of steam and CO_2 gasification reactions. They further added that due to increased char particle temperature in the oxygen-enriched atmosphere, the char consumption shows a strong dependency on gasification reactions. Niu et al[108] proposed a new model of pulverized coal char particle burnout that considers both ash dilution and ash film inhibition of char burnout. They also evaluated the impact of different modes of ash inhibition by comparing experimental data on char combustion and burnout. They emphasized on including char oxidation along with steam gasification reaction to obtain good agreement with measured data. The model results showed that ash dilution has a negligible effect on the char combustion process for low to intermediate burnout levels. They further added that for higher burnout levels, the char combustion process is strongly dependent on both the ash dilution and ash film inhibition due to high ash content and effective internal particle diffusion on char burning rate. Niu et al[109] developed an intrinsic char kinetics model which considers the ash effects (such as ash film formation, ash dilution, and ash vaporization), both gasification and oxidation, homogeneous nucleation of particles, heterogeneous condensation of vapor, mechanisms of coalescence, and coagulation. The model is used for calculation of the temporal evolution of nanoparticle number and size in both O_2/N_2 and O_2/CO_2 combustion environments for char particle having different size and ash content. They reported that both formation and growth of nanoparticles is strongly dependent on the char combustion temperature and high char combustion temperature enhances the rate of mineral vaporization within the particle of char subsequently increasing the rates of nucleation and condensation. High local char burning temperature is promoted by small size char particles, high oxygen content, and low ash content which shifts the size distribution of nanoparticle to larger sizes. Both the size of nanoparticle formed and number density are lower in the O_2/CO_2 environment than the O_2/N_2 environment. Niu et al[110] extended their previous efforts to model the formation of ultrafine particle employing the Char Burning and Particulate Matter Kinetics (CBPMK) model, during char combustion, and investigated the influence of various FGR parameters such as FGR rate, the size distribution of particles, and dust removal efficiency. They observed that the FGR without recirculated particles results in the nucleation of fewer but larger particles. They reported reduced particle collision frequency by diluting FGR gases, which is the main cause of high number density and small particle size after coalescence. They further added that the recirculation of particles provides surface area for condensation of mineral vapor which promotes the formation of fewer, but larger nuclei and reduces saturation of mineral vapor. Sun and Hurt[111] developed a model (CBK version 8) to

ISSN NO: 9726-001X
Volume 10 Issue 03 2022

examine the mass and energy transport that governs char particle temperature and explains the extinction phenomenon during char particle combustion. Their model accurately predicted extinction phenomenon during combustion of pulverized coal char and in agreement with available data. Unburnt carbon (UBC) had a strong dependency on temperature, oxygen concentration, and particle residence time. The plant operating conditions attributed to the increase in UBC. Reduced thermal efficiency and low removal efficiency of physical precipitators were attributed due to high UBC in ash. Unburnt carbon (UBC) has the potential to retain mercury in the fly ash and creates ash saleability issues. Prediction of UBC by the standard model was limited only to air fired condition where the concentration of CO_2 and steam was low.

To clarify the effect of CO_2 gasification reaction on overall char conversion in oxy-fuel combustion environment, Kim et al[112] performed burnout simulation of coal char particle in oxy-fuel combustion conditions. Reactivity of char and single film model including Stefan flow effect on mass and energy transfer was adopted in their simulation. They performed burnout simulation study in the air (21% O_2), oxy-fuel (30% O_2), and oxygen-deficient (5% O_2) combustion conditions. The simulation results showed that the char particle temperature is reduced by endothermic gasification reaction which is the main cause of reduced oxidation rates. They reported that the char burnout time and relative carbon consumption are greatly influenced by gasification reaction in oxygen-deficient combustion conditions. They concluded that the effect of CO_2 gasification reaction was dependent on temperature, particle size, gas composition, and kinetic parameters. Niu et al[113] studied the char conversion characteristics in DTF at 1373 K at various O_2 and CO_2 content. Figure 9 shows that the minimal conversion point corresponds to 9 to 13 vol. % CO_2 content. At minimal conversion point, promotion effect of CO_2 gasification reaction catches up with the suppression effect. They reported the occurrence of the inflection point (at around 17-25 vol % CO_2) where the promotion effect of CO_2 gasification reaction surpasses the suppression effect. They further added that an increase in O_2 content shifts both the points towards high CO_2 content. The effect of the increase in combustion gas temperature had inverse trend compared with the increase in O_2 content. Gonzalo-Tirado et al[114] reported enhanced overall char conversion rate due to CO_2 gasification reaction in 4 and 21 vol% O_2 in N_2 and CO_2 at 1573 K employing single film model.

Geier et al[115] studied the effect of both CO_2 and steam gasification reactions on char combustion employing single-film model. They reported that the char particle

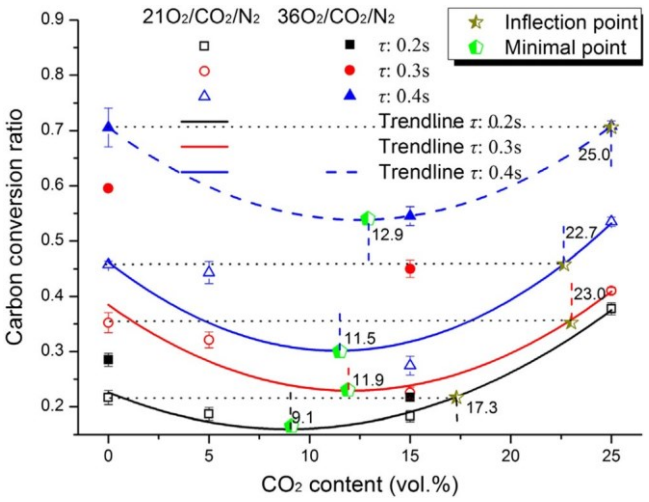

FIGURE 9 Char conversion ratio under various $O_2/CO_2/N_2$ atmospheres and residence times τ[113] [Colour figure can be viewed at wileyonlinelibrary.com]

temperature was predicted accurately in 12 to 36 vol% O_2 in N_2 and CO_2 at 1680 K. Huang et al[116] performed experimental investigation of bituminous coal combustion in O_2/CO_2 atmosphere and reported that the suppression effect of CO_2 gasification reaction is stronger than the promotion effect of CO_2 gasification reaction on char consumption.

The reactions of char combustion can be studied by various available models. Each model has its own benefits and limitations. The diffusion-limited reaction rate model assumes that the surface reaction proceeds at a rate determined by the diffusion of gaseous oxidant to the surface of the particle. This model ignores the effect of kinetic rate on surface reaction. The kinetic/diffusion-limited rate model assumes the surface reaction rate of char is dependent on both kinetic and diffusion rates. The char characteristics during combustion are assumed to be constant in both of the diffusion-limited rate model and the kinetic/diffusion-limited rate model. As these models are based on char external area, they do not consider particle swelling, char porosity, diffusion of oxygen, and internal reactions.[4] The char burnout is greatly influenced by the surface area of char and pores and their effect on diffusion, so these effects cannot be ignored. Smith[117] considered these effects in his intrinsic char combustion model formulation so that the char combustion can occur in the internal pores of the particle. The Carbon Burnout Kinetic model of Hurt et al[118] is variant of intrinsic model specially developed to predict carbon burnout and ultimate fly ash carbon content for prescribed temperature/oxygen history. This model also considers the Stefan flow effect on char combustion. Char reaction is slowed down due to Stefan flow effect. Stefan flow also reduces the particle surface temperature by

ISSN NO: 9726-001X
Volume 10 Issue 03 2022

reducing heat transfer to the char particle and accelerating heat transfer from the char particle, which results into delayed char reaction. A summary of commonly used char combustion models is shown in Table 5.

2.10 | Emissions from pulverized coal furnaces

Coal combustion is not environment-friendly as it produces pollutants such as oxides of nitrogen (NO_x), oxides of sulfur (SO_x), SPM, and mercury etc. This section insights the emissions from pulverized fired furnaces.

Figure 10 shows the effect of fuel blending on emission characteristics in both air and oxyfuel combustion conditions, reported by Moroń and Rybak.[119] They reported reduced NO_x and SO_2 emission due to the blending of biomass with coal. The similar effect of fuel blending on NO_x and SO_2 emission was also reported by Riaza et al.[19] Backreedy et al[120] reported reduced NO concentration for the coal blends than single coal. CO_2, NO_x, and SO_2 emission characteristics in both air and oxy-fuel combustion conditions were investigated by Chen et al.[121] They found 90% higher CO_2 concentration in the flue gas in oxy-fuel conditions than air combustion condition. Thus, under oxy-fuel combustion conditions, CO_2 can be easily separated by various CCS technologies and greenhouse gas emission can be reduced. They reported reduced NO_x under oxy-fuel combustion conditions due to the reduced flame temperature in the oxy-fuel conditions. Reduced NO_x emission by flue gas recycling is also reported by Hjärtstam et al.[16] Hu et al[122] experimentally studied the NO_x emission characteristics under oxy-fuel combustion conditions in upward flow coal combustor operating at low RR. The result showed that the increase in equivalence ratio decreases NO_x emission. They found increase in NO_x emission with an increase in RR. They concluded that the NO_x emission had a strong dependency on nitrogen release rate into the volatile matter and ratio of volatile N to char N. Gaikwad et al[76] investigated the effect of combustion environment on NO concentration and temperature in their 2D simulation in the swirl burner as shown in Figure 11. They found the lowest NO concentration in the oxy-steam environment (obtained by replacing N_2 or CO_2 with H_2O). Belošević et al[123] investigated the effect of furnace sorbent injection

TABLE 5 Summary of commonly used char combustion model[73]

Model Description	Merits/Limitations	Author(s)
· Apparent activation energy-based model assumes that burning of char takes place at constant diameter.	· Being a global model, it cannot address the effect of coal swelling and consequent change in particle diameter during combustion.	Baum and street[89]
· Char combustion is controlled by chemical reaction only (diffusion is neglected)	· The model parameters need to be derived for every coal type.	
· Intrinsic reactivity-based model assumes that the burning of char takes place at constant density.	· Has potential to provide coal generic kinetic rate constants.	Smith[117]
· Char combustion is controlled by both chemical reaction and diffusion.	· This model does not account for varying effectiveness of combustion due to dependency on average char surface area.	
· Carbon Burnout Kinetic (CBK) and its variants.	· This model considers the effects of rank dependence, char deactivation, and ash inhibition during char combustion process thus making it more realistic.	Sun and Hurt[111]
· Based on constant char surface area.	· Overprediction of burnout due to constant char surface area	

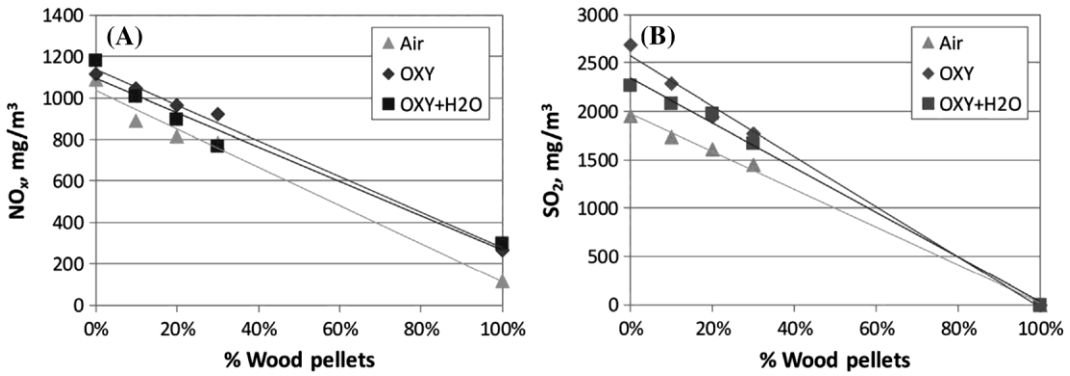

FIGURE 10 Variation of (A) NO_x and (B) SO_2 emission with varying content of wood pellets under different atmospheres[119]

ISSN NO: 9726-001X
Volume 10 Issue 03 2022

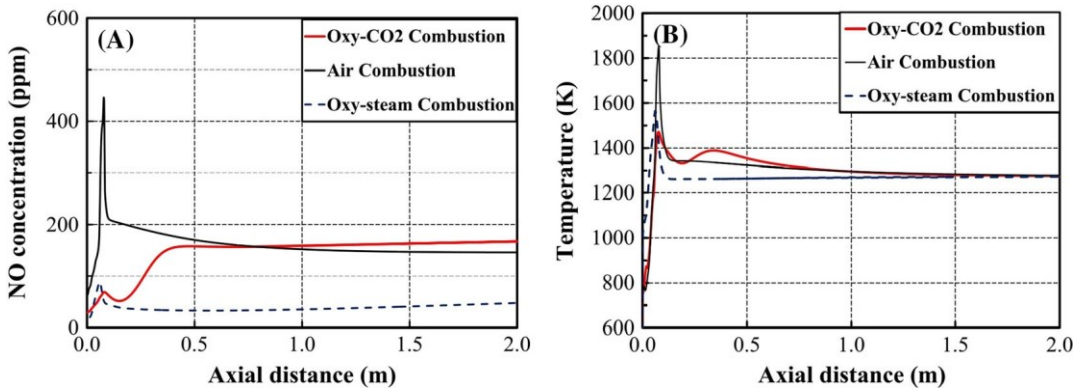

FIGURE 11 Effect of combustion environment on (A) NO concentration and (B) temperature along the furnace axis[76] [Colour figure can be viewed at wileyonlinelibrary.com]

(FSI) and different combustion modifications in 350 MW boiler tangentially fired furnace on SO_2 and NO_x emission. They reported that SO_2 emission reduced with an increase in sorbent flow rate. However, an excessive value of sorbent flow rate is to be avoided. They observed that fine grinded sorbent particles are more efficient and produced a better de-SO_2 effect. They obtained maximum SO_2 reduction (around 56%) when 50% of the sorbent injected through and 50% above the burners. They further added that the NO_x emission could be reduced by the boiler exit FGR economically and effectively.

Adamczyk et al[124] investigated the effect of the reburning process of gasification gas obtained from sewage sludge on NO_x emission employing computational modeling in the large-scale boiler. They reported that the injection location along with syngas injected affects the NO_x emission in the boiler. They obtained reduced NO_x emission when secondary fuel proportion was increased from 10% to 20%. They observed better efficiency by injecting syngas through overfire air (OFA) nozzles than through the last row of burners. Bohnstein et al[125] proposed a model of sulfur release on the basis of the transformation of mineral matters of sulfur-bearing minerals in pulverized coal combustion and measured concentrations of gases at various heights, radial distances, and exit of the combustor. They observed maximum temperature (1975 K) immediate below of the burner where pyrolysis reactions and releases of volatile matter occur. They obtained SO_2 emission level of 350 ppm beneath the burner.

Kurose et al[58] investigated how ash content in coal affects combustion properties in staged combustion conditions. They tested three coals having 36, 44, and 55 wt% of ash contents. They reported that by increasing ash content in coal, NO_x formation slowed down adjacent to burner and concentration of NO_x increased at the furnace exit. Costa et al[126] measured O_2, CO_2, NO_x, and CO concentrations at various ports of the 300 MW front wall-fired boiler and found low NO_x burner produced the higher concentration of CO. They reported the maximum measured NO_x concentration of 445 ppm obtained at 2.4 m from the side wall at port 5. Ribeirete and Costa[127] reported reduced NO_x by reducing primary zone stoichiometric ratio (λ_{pz}). They observed that the NO_x emission has less dependency on staged air injector configuration. Shen et al[128] carried out the combustion of superfine anthracite coal to investigate the NO_x emission characteristics in the single and multi-air staged atmosphere. They reported that superfine coal particles have 12% to 22% more NO_x reduction efficiency than regular sized particles and NO_x reduction in multi-staged combustion was more than that in the single staged atmosphere. Chen et al[129] investigated the effect of stoichiometric ratio on NO_x emission and reported that the decrease in the stoichiometric ratio (SR) from 1.0 to 0.6, reduced the NO concentration from 661.89 mg/N-m^3 to 169.99 mg/N-m^3. Wielgosinski et al[130] determined pollutant emissions such as carbon monoxide (CO), nitrogen oxide (NO), and hydrocarbons generated during biomass combustion. They compared emission level obtained using biomass as fuel with using fine coal as reference fuel. They found organic compound emission much higher than the hard coal. They concluded that the emission intensity of biomass fuel is far too high and comparable to those in coal combustion. Thus, biomass is undoubtedly renewable fuel, but it is not ecological.

Pulverized coal combustion is the main source of various emissions such as greenhouse gases, NO_x, SO_x, and particulate matter, etc. Continuous efforts were made to control these emissions. As far as NO_x emission is concerned, it is dependent on various factors such as fuel type, the volatile content of the fuel, furnace, and burner configuration.[55] NO_x emission can be controlled by modifying the combustion process. These modifications include utilization of low NO_x burner, furnace air staging, flue gas recirculation, reburning of fuels, and process

ISSN NO: 9726-001X
Volume 10 Issue 03 2022

optimization. These combustion modifications can easily be implemented on new boilers, whereas for existing ones these modifications are tough to implement.

Sulfur dioxide emission from pulverized fired furnaces can be controlled by switching to a fuel containing less sulfur, by removing sulfur bearing components by proper cleaning of coal and by installing flue gas desulphurization system (FGD). In the present scenario, FGD has gained a lot of interest to control SO_x emission from pulverized fired furnaces. FGD technology can be broadly classified as wet or dry depending upon the nature of by-products generated.[131]

Greenhouse gases emitted during combustion of pulverized coal are the major cause of global warming. Carbon capture and sequestration (CCS) technologies are trending measure to control greenhouse gases emission. Detailed discussion on CCS technologies is given in Section 2.11.

2.11 | Carbon capture and sequestration

Increasing concentration of CO_2 is the environmental concern and main cause of global warming. Only CO_2 itself is responsible for around 60% of the global warming.[13,132] Atmospheric CO_2 concentration can be reduced by (1) utilizing energy more efficiently, (2) utilizing alternative fuel and renewable energy, and (3) CCS technologies. The CO_2 capture and sequestration approaches are (1) pre-combustion capture, (2) post-combustion capture, and (3) oxy-fuel combustion capture. In pre-combustion capture, syngas is produced from gasification of fossil fuel; then, syngas is converted into CO_2 and H_2 in water shift reaction. CO_2 can be separated, and hydrogen-rich syngas is fed to combined power generation cycle. In post-combustion capture, CO_2 is captured from flue gas after the combustion of fossil fuels. In post-combustion capture, chemical solvents are utilized for CO_2 capture. In oxy-fuel combustion capture, fuel is burnt in pure oxygen and RFG. The high concentration CO_2 is captured from flue gas by condensing water vapor. The schematic diagram of these CO_2 capture and sequestration approaches are shown in Figure 12–14.

International Energy Agency (IEA) claimed in its roadmap that 20% of the total CO_2 emission would be removed through CCS by 2050. Many authors reported that all CCS methods result in reduced plants efficiency.

Pre-combustion and post-combustion capture results in the decrease of plant efficiency by around 8% to 12%, whereas in oxyfuel combustion capture plant efficiency reduction (around 7%-11%) is little low due to heat integration and process optimization. CCS technologies are very expansive and lack its application in industrial units. The capture of CO_2 is the most expansive part of CCS and accounts for around 75% of the total CCS cost.

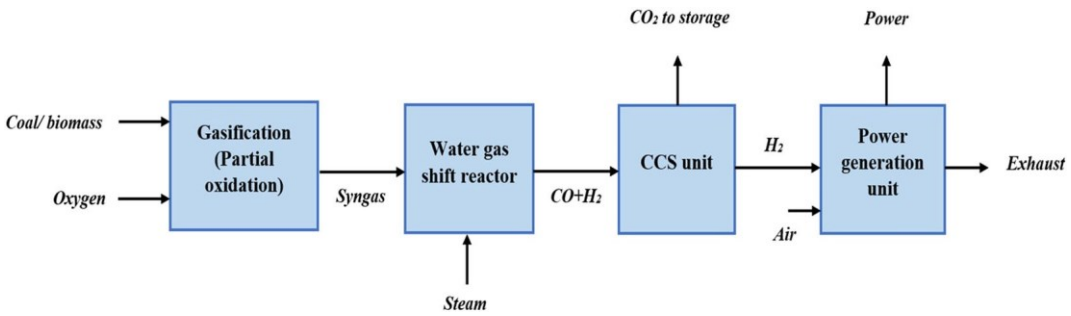

FIGURE 12 Schematic diagram of pre-combustion capture (adapted from Mondal et al[133]) [Colour figure can be viewed at wileyonlinelibrary.com]

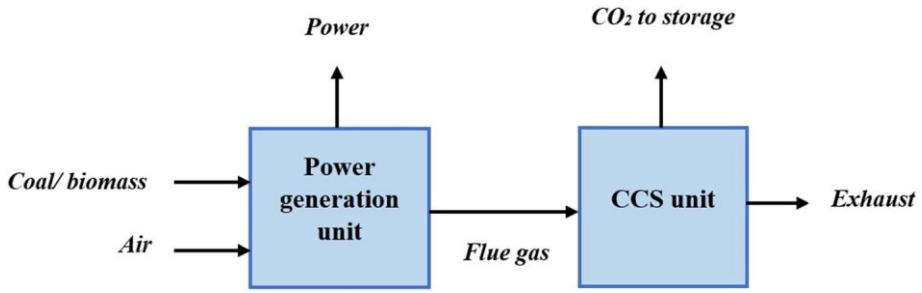

FIGURE 13 Schematic diagram of post-combustion capture (adapted from Zou et al[134]) [Colour figure can be viewed at wileyonlinelibrary.com]

ISSN NO: 9726-001X
Volume 10 Issue 03 2022

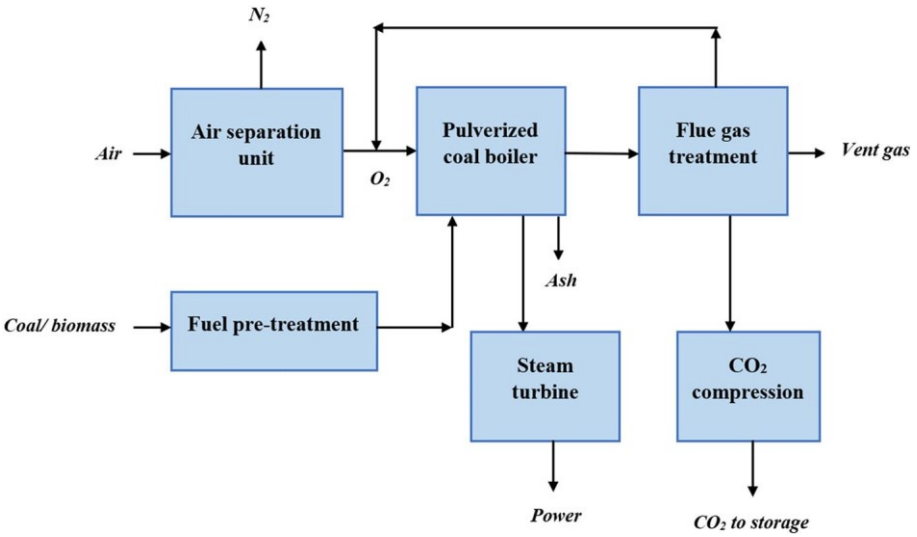

FIGURE 14 Schematic diagram of oxy-fuel combustion capture (adapted from Cormos[137]) [Colour figure can be viewed at wileyonlinelibrary.com]

Pettinau et al[135] presented the comparison between the integrated gasification combined cycle (IGCC) and ultra-supercritical pulverized coal combustion (USC) plants. They employed three configurations: a CO_2 free configuration, a configuration without CCS, and a partial capture configuration (CCS system is employed to the portion of produced gas). They reported IGCC was more effective for the CO_2 free configuration, whereas USC technology was profitable for without CCS configuration. Escudero et al[136] developed a methodology for the reduction of the energy penalty of the oxy-fuel combustion system coupled with CCS technology. They optimized the air separation unit (ASU) and compression and purification unit (CPU) for the lower energy consumption of a boiler operating at high oxygen concentration. They reported the increase in the net efficiency of power plant (36.42%) with respect to reference oxy-fuel power plant (32.91%). They further added that this leads to a decrease in the energy penalty from 10.5 points to 7.3 points.

Cormos[137] presented the in-depth techno-economic analysis of the oxy-fired power plant which generates 350 MW power with CO_2 capture rate higher than 90%. He operated the same supercritical power plant without CCS for the estimation of energy penalty, capital, operating, and maintenance cost. He reported the increase in the energy penalty and capital cost by 9% to 12% and 37% to 50%, respectively, with CCS. He further added that electricity cost and operating and maintenance costs were increased by 54% to 95% and 7% to 15%, respectively. Soundararajan and Gundersen[138] designed pressurized oxy-fuel combustion system for CO_2 capture. They reported the increase in power output and reduction in auxiliary power consumption of the pressurized supercritical cycle by 18 and 10 MW, respectively. They obtained efficiency enhancement in the order of 1.7% and improvement in CO_2 recovery factor by 2.8% to 97.8%. Garg et al[139] examined the large point sources of CO_2 emissions in India and updated CO_2 emission estimates in various intense energy consuming sectors such as power, cement, steel, fertilizer, and refinery. They matched emissions from large point sources with the nearest CO_2 storage locations across India. Their computational method estimated the storage locations for each CO_2 emitting source by considering the storage capacity of each location. Integration of evaporative gas turbine (EvGT) cycle with oxy-fuel combustion was investigated by Hu et al[140] for CO_2 capture. In their investigation, they found that the system's electrical efficiency was affected by the purity of oxygen and the ratio of water/gas (W/G). They compared the performance of both dry and wet recycled oxy-fuel combustion. They found that 97% oxygen purity has maximum electrical efficiency. They observed the existence of an optimum value of W/G for both EvGT and integrated EvGT with oxy-fuel combustion CO_2 capture technology. They further added that maximum electrical efficiency corresponds to the maximum temperature difference between the stack temperature and humid gas temperature after recuperator (HGT). They reported dry recycle oxy-fuel combustion more efficient than the wet recycle oxy-fuel combustion. Exergy analysis of post-combustion CO_2 capture combined-cycle power plant of natural gas was performed by the Amrollahi et al.[141] They reported exergy efficiency and energy efficiency penalties of 3.6% points and 7.1% points, respectively, when CO_2 capture unit was added to the combined-cycle power plant of natural gas. Exergy efficiency of CO_2 capture and compression units were 21.2% and 67% making the overall effective efficiency of

ISSN NO: 9726-001X
Volume 10 Issue 03 2022

TABLE 6 Diagnostic system for coal combustion

S. N.	Property	Measuring Instruments	Ref.
1	Velocity	Laser doppler velocimetry	Heil et al[154]
		Laser doppler anemometry (LDA)	Toporov et al[17]
		Shadow doppler particle analyzer (SDPA)	Cai et al[152]
		Laser doppler velocimetry (LDV)	Cai et al[152]
2	Gas temperature	R type thermocouple	Kim et al[155]
		Suction pyrometer	Weidmann et al[156]
		Bichromatic pyrometer (IMPAC ISR 12-LO)	Zellagui et al[157]
		K type thermocouple	Zellagui et al[157]
		Three color optical pyrometer	Maffei et al[158]
		Suction pyrometer	Hjärtstam et al[16]
		Water-cooledsuction pyrometer	Sadiki et al[71]
3	Temperature distribution inside furnace	Acoustic gas temperature measuring (AGAM)	Modliński et al[159]
4	Coal particle temperature	Two-color pyrometer	Toporov et al[17]
		S type thermocouple	Zellagui et al[157]
		Radiation thermometer(OS3753)	Guo et al[26]
5	Ultimate analysis	CHNS analyzer (EL-2 Vario)	Shen et al[128]
		CHNS analyzer	Kazagic and Smajevic[46]
6	Radiative heat flux	Ellipsoidal radiometer	Weidmann et al[156]
		Meditherm radiation heat flux meter	Smart et al[20]
7	Convective heat flux	In-house designed convective probe	Smart et al[20]
8	Grinding of coal/biomass	Ball mill	Tamura et al[160]
		Vertical roller mill	Tamura et al[160]
		Vibration mill	Tamura et al[160]
		Centrifugal mill	Zellagui et al[157]
		Jaw crusher	Sahu et al[161]
10	Spontaneous emission ofexcited OH-molecules	CCD camera	Hees et al[15]
		FASTCAM SA4 high-speedcamera	Kim et al[155]
		Chemiluminescence imaging	Weidmann et al[156]
11	Exhaust gas analysis	NDIR (non-dispersive infrared spectrography)	Hees et al[15]
		FTIR (Fourier transform infrared spectroscopy)	Vekemans et al[56]
		Gasmet DX2000 FTIR analyzer	Weidmann et al[156]
		Spectrum analyzer	Moroń and Rybak[119]
		Testo 350 M gas analyzer	Chen et al[129]
		FTIR Gasmet DX4000	Shen et al[128]
		NDIR Analyzer	Hjärtstam et al[16]
		Gas analyzer (Testo350)	Kazagic and Smajevic[46]
		Horiba PG-350 flue gas analyzer	Guo et al[26]
		FTIR analyzer	Marek and Światkowski[162]
12	Hydrocarbon measurement	Flame ionization detector	Ribeirete and Costa[127]
13	Oxygen concentration	Magneto mechanical analyzer	Toporov et al[17]
14	NO and NO_2 concentration	UV photometer	Toporov et al[17]
15	CO_2 and CO concentration	NDIR	Toporov et al[17]
16	Particle size	Malvern Mastersizer 3000	Ndibe et al[55]
		Malvern Mastersizer 2000	Chen et al[129]

(Continues)

ISSN NO: 9726-001X
Volume 10 Issue 03 2022

TABLE 6 (Continued)

S. N.	Property	Measuring Instruments	Ref.
		Malvern Mastersizer 3000	Moroń and Rybak[119]
		Malvern Mastersizer 5004	Shen et al[128]
17	Petrographic measurements	Polarized light microscope	Sahu et al[161]
		Simultaneous ThermalAnalyzer (model: STA 449F3 Jupiter, NETZSCH, Germany),	Sahu et al[161]
18	Thermogravimetric analysis	Mettler Toledo TGA/SDTA 851 apparatus	Magdziarz and Wilk[163]
19	Morphology of coal samples	XRF technique	Moghtaderi[164]
		SEM	Meesri and Moghtaderi[165]
		XRF	Meesri and Moghtaderi[165]
20	Size distribution of the raw coal	Computer controlled scanning electron microscopy (CCSEM)	Beckmann et al[59]
		Wet laser diffraction	Beckmann et al[59]
		Dry laser diffraction	Beckmann et al[59]
		Sieve analysis	Beckmann et al[59]
21	Viscosity	Viscometer	Beckmann et al[59]

CO_2 capture and compression unit around 31.6%. They observed that the exergy loss in CO_2 capture and compression unit was comparatively smaller than that of the gas turbine unit.

3 | DIAGNOSTIC SYSTEM OF COAL COMBUSTION

The list of instruments used for diagnostics of coal combustion are as follows in Table 6.

4 | CHALLENGES, OPPORTUNITIES, AND FUTURE RESEARCH DIRECTIONS

In conventional air-fired furnaces, high amount of nitrogen is heated during combustion and then cooled down again during the release of exhaust gas. The temperature of exhaust gas is more than the ambient temperature. Thus, around 10% of heat is lost in air-fired boilers. Whereas in oxy-fuel furnaces exhaust gas does not have nitrogen in bulk quantity, which in turn reduces the mass and volume of exhaust flue gas. This is the main reason for reduced heat loss with flue gas and improved heat efficiency of the boiler under oxy-fuel conditions.

Oxy-fuel boilers make use of pure oxygen as oxidizer. Thus, another major opportunity of oxy-fuel combustion is to control and optimize the pulverized coal combustion process by adjusting the amount of O_2 injected into the furnace and its injection location. Furthermore, with oxy-fuel combustion, near zero emission level can be obtained. The absence of N_2 in oxidizer reduces the NO_x emission level, and after condensing water vapor of exhaust gas, highly concentrated CO_2 can be separated (exhaust gas mainly has CO_2 and water vapor in oxy-fuel combustion).

As far as challenges of oxy-fuel technology are concerned, it has mainly technical and economic challenges. Technical challenges include boiler design and system operations, whereas economic challenges include the high energy cost of O_2 production and CO_2 separation.

Co-firing of biomass with coal can serve as a renewable energy source, and co-firing has been proved environment-friendly due to minimized greenhouse gases (GHGs) and other emissions. Co-firing has potential opportunities in agricultural, constructional, manufacturing, transportation, and food processing industries to manage combustible agricultural and wood wastes. However, co-firing is associated with few technical challenges such as quality of biomass, the proportion in which biomass to be added with coal, deposit formation, corrosion, and boiler performances. Another major challenge of biomass is its unreliability due to unstable supply of biomass.

The challenges and research need in other aspects of pulverized coal combustion are summarized below.

- There is a need for extensive numerical modeling to incorporate the recent advancement of submodels and to consider the highly relevant minor species in pulverized fired furnaces.

- Both gas phase and particle phase characteristics alter significantly at elevated pressure. Heat and mass transfer, gas phase, and char combustion kinetics are still unknown at elevated pressure.
- Many authors have investigated emission characteristics under air and oxy-fuel environment, but there is a lack of studies on ash behavior and slagging particularly in the oxy-fuel environment. There is a need for a thorough study on coagulation, phase changes, element partitions, and size distribution in the oxy-fuel atmosphere.
- Since radiation is the dominant mode of heat transfer in coal combustion furnaces, better turbulence-radiation and gas emission/absorption submodels are necessary to improve the prediction of the temperature field.
- There is a need for in-depth techno-economic analysis for the optimization of the oxy-fired power plant and CCS technologies for the improvement of efficiency and reduction of energy penalty and capital cost.
- Due to incomplete understandings of advanced combustion technologies such as IGCC and chemical looping combustion, it is necessary to pay more attention to these technologies.

5 | CONCLUSIONS

Several facets of coal combustion have been emphasised in this study, including oxy-fuel combustion, co-combustion of coal and biomass, emissions from pulverised coal furnaces, ash production and deposition, and CCS technology. We go over the fundamentals of pulverised coal combustion and how to simulate pulverised coal furnaces using computational fluid dynamics (CFD). The following is a summary of the main findings.

• Under oxy-fuel combustion conditions, reaction pathways and combustion characteristics undergo substantial changes as a result of distinct physical and chemical features.

to less nitrogen than carbon dioxide.

Oxy-fuel combustion varies from air combustion in various aspects, including delayed flame ignition, according to both experimental and numerical research.

changes to heat transport, decreased emissions, associated flame instability, and tion.

Co-firing biomass and coal produces renewable energy.

accessible energy sources and offers a number of advantages, including less emissions of harmful gases like CO2, NOx, and SOx. The main reason for the reduction of NOx and SOx is that biomass contains very little sulphur and very little nitrogen.

released gas. During its development, biomass absorbs carbon dioxide, and when burned, it releases it. So, the atmospheric CO2 level is stable.

• It is clear from the review that fuel blend-

Lowering emissions of sulphur dioxide and nitrogen oxides is achieved via ing. In addition to lowering NO emissions, lowering the local

ratio of oxygen to fuel. The addition of biomass to coal and the oxy-fuel atmosphere resulted in a decrease in NO emissions. Addiction is shown by NO decrease efficiency.

according to the fuel recycling and equivalency ratios. Because water is used instead of carbon dioxide or nitrogen in the oxy-steam combustion environment, NO emissions are also reduced.

atmosphere).

• The efficiency of plants is diminished as a consequence of carbon capture and sequestration (CCS) technology. An 8% to 12% decrease in plant efficiency is seen for both pre- and post-combustion capture, whereas the decrease in efficiency for the

7–11% of oxyfuel combustion is captured. Carbon capture and sequestration (CCS) units have a 9% to 12% increase in capital cost and a 7% to 15% increase in maintenance cost.

• The mechanisms of transport and chemical reactions are the

combustion of ground coal produces principal causes of irreversibility.

REFERENCES

1. Barnes DI. Understanding pulverised coal, biomass and waste combustion—a brief overview. *Appl Therm Eng*. 2015;74:89-95.
2. Chen L, Yong SZ, Ghoniem AF. Oxy-fuel combustion of pulverized coal: characterization, fundamentals, stabilization and CFD modeling. *Prog Energy Combust Sci*. 2012;38(2):156-214.
3. Scheffknecht G, Al-Makhadmeh L, Schnell U, Maier J. Oxy-fuel coal combustion—a review of the current state-of-the-art. *Int J Greenh Gas Control*. 2011;5:16-35.
4. Edge P, Gharebaghi M, Irons R, et al. Combustion modelling opportunities and challenges for oxy-coal carbon capture technology. *Chem Eng Res Des*. 2011;89(9):1470-1493.
5. Wall T, Liu Y, Spero C, et al. An overview on oxyfuel coal combustion—state of the art research and technology development. *Chem Eng Res Des*. 2009;87(8):1003-1016.
6. Yin C, Yan J. Oxy-fuel combustion of pulverized fuels: combustion fundamentals and modeling. *Appl Energy*. 2016; 162:742-762.
7. Tabet F, Gökalp I. Review on CFD based models for co-firing coal and biomass. *Renew Sustain Energy Rev*. 2015;51:11 01-1114.

8. Agbor E, Zhang X, Kumar A. A review of biomass co-firing in North America. *Renew Sustain Energy Rev*. 2014;40:930-943.
9. Nemitallah MA, Habib MA, Badr HM, Said SA. Oxy-fuel combustion technology: current status, applications, and trends. *Int J Energy Res*. 2017;41(12):1670-1708.
10. Mathekga HI, Oboirien BO, North BC. A review of oxy-fuel combustion in fluidized bed reactors. *Int J Energy Res*. 2016;40(7):878-902.
11. Borah RC, Ghosh P, Rao PG. A review on devolatilization of coal in fluidized bed. *Int J Energy Res*. 2007;31:135-147.
12. Habib MA, Badr HM, Ahmed SF, Mezghani K, Imashuku S. A review of recent developments in carbon capture utilizing oxy-fuel combustion in conventional and ion transport membrane systems. 2011;35:741-764.
13. Cau G, Tola V, Ferrara F, Porcu A, Pettinau A. CO_2-free coal-fired power generation by partial oxy-fuel and post-combustion CO_2 capture: techno-economic analysis. *Fuel*. 2018;214:423-435.
14. Toporov DD. Combustion of pulverised coal in a mixture of oxygen and recycled flue gas. 2014.
15. Hees J, Zabrodiec D, Massmeyer A, Habermehl M, Kneer R. Experimental investigation and comparison of pulverized coal combustion in CO_2/O_2- and N_2/O_2-atmospheres. *Flow, Turbul Combust*. 2016;96(2):417-431.
16. Hjärtstam S, Andersson K, Johnsson F, Leckner B. Combustion characteristics of lignite-fired oxy-fuel flames. *Fuel*. 2009;88 (11):2216-2224.
17. Toporov D, Bocian P, Heil P, et al. Detailed investigation of a pulverized fuel swirl flame in CO_2/O_2 atmosphere. *Combust Flame*. 2008;155(4):605-618.
18. Jovanović R, Rašuo B, Stefanović P, Cvetinović D, Swiatkowski B. Numerical investigation of pulverized coal jet flame characteristics under different oxy-fuel conditions. *Int J Heat Mass Transf*. 2013;58(1-2):654-662.
19. Riaza J, Gil MV, Álvarez L, Pevida C, Pis JJ, Rubiera F. Oxy-fuel combustion of coal and biomass blends. *Energy*. 2012; 41(1):429-435.
20. Smart JP, O'Nions P, Riley GS. Radiation and convective heat transfer, and burnout in oxy-coal combustion. *Fuel*. 2010;89 (9):2468-2476.
21. Bhuiyan AA, Naser J. CFD modelling of co-firing of biomass with coal under oxy-fuel combustion in a large scale power plant. *Fuel*. 2015;159:150-168.
22. Zhou Y, Jin X, Jin Q. Numerical investigation on separate physicochemical effects of carbon dioxide on coal char combustion in O_2/CO_2 environments. *Combust Flame*. 2016; 167:52-59.
23. Liu J, Liu Z, Chen S, Ong S, Zheng C. International Journal of Greenhouse Gas Control A numerical investigation on flame stability of oxy-coal combustion: Effects of blockage ratio, swirl number, recycle ratio and partial pressure ratio of oxygen. *Int J Greenh Gas Control*. 2017;57:63-72.
24. Chae T, Yang W, Ryu C. Investigation of flame characteristics using various design parameters in a pulverized coal burner for oxy-fuel retrofitting. *Int J Energy Res*. 2018;41:3206-3217.
25. Smart JP, Patel R, Riley GS. Oxy-fuel combustion of coal and biomass, the effect on radiative and convective heat transfer and burnout. *Combust Flame*. 2010;157(12):2230-2240.
26. Guo J, Liu Z, Huang X, et al. Experimental and numerical investigations on oxy-coal combustion in a 35 MW large pilot boiler. *Fuel*. 2017;187:315-327.
27. Rebola A, Azevedo JLT. Modelling pulverized coal combustion using air and O_2^+ recirculated flue gas as oxidant. *Appl Therm Eng*. 2015;83:1-7.
28. Nakod P, Krishnamoorthy G, Sami M, Orsino S. A comparative evaluation of gray and non-gray radiation modeling strategies in oxy-coal combustion simulations. *Appl Therm Eng*. 2013;54(2):422-432.
29. Corrêa Da Silva R, Krautz HJ. Experimental studies on heat transfer of oxy-coal combustion in a large-scale laboratory furnace. *Appl Therm Eng*. 2015;82:82-97.
30. Li D, Liu X, Xu K, Zha Q, Lv Q. Numerical study on combustion and heat transfer properties under oxy-fuel condition in a 600MW utility boiler. *Energy Procedia*. 2017;105:4009-4014.
31. Sahu SG, Chakraborty N, Sarkar P. Coal-biomass co-combustion: an overview. *Renew Sustain Energy Rev*. 2014; 39:575-586.
32. Saidur R, Abdelaziz EA, Demirbas A, Hossain MS, Mekhilef S. A review on biomass as a fuel for boilers. *Renew Sustain Energy Rev*. 2011;15(5):2262-2289.
33. Lu J, Chen W. Investigation on the ignition and burnout temperatures of bamboo and sugarcane bagasse by thermo gravimetric analysis. *Appl Energy*. 2015;160:49-57.
34. Liu Z, Hu W, Jiang Z, Mi B, Fei B. Investigating combustion behaviors of bamboo, torrefied bamboo, coal and their respective blends by thermogravimetric analysis. *Renew Energy*. 2016;87:346-352.
35. Moon C, Sung Y, Ahn S, Kim T, Choi G, Kim D. Thermochemical and combustion behaviors of coals of different ranks and their blends for pulverized-coal combustion. *Appl Therm Eng*. 2013;54(1):111-119.
36. Sarkar P, Sahu SG, Mukherjee A, et al. Co-combustion studies for potential application of sawdust or its low temperature char as co-fuel with coal. *Appl Therm Eng*. 2014;63(2):616-623.
37. Elorf A, Koched N, Boushaki T, Sarh B, Bostyn S, Gökalp I. Swirl motion effects on flame dynamic of pulverized olive cake in a vertical furnace. *Combust Sci Technol*. 2016;188(11-12): 1951-1971.
38. Liang F, Wang R, Jiang C, et al. Investigating co-combustion characteristics of bamboo and wood. *Bioresour Technol*. 2017;243:556-565.
39. Ghenai C, Janajreh I. CFD analysis of the effects of co-firing biomass with coal. *Energ Conver Manage*. 2010;51(8):16 94-1701.
40. Al-Widyan MI, Tashtoush G, Hamasha AM. Combustion and emissions of pulverized olive cake in tube furnace. *Energ Conver Manage*. 2006;47(11-12):1588-1596.
41. Bhuiyan AA, Naser J. Computational modelling of co-firing of biomass with coal under oxy-fuel condition in a small scale furnace. *Fuel*. 2015;143:455-466.

42. Bhuiyan AA, Naser J. Thermal characterization of coal/straw combustion under air/oxy-fuel conditions in a swirl-stabilized furnace: A CFD modelling. *Appl Therm Eng*. 2016;93:639-650.

43. Lv Q, Xuan W, Yongbo L, Debo D, Defu L. Combustion and heat transfer characteristics of co-firing biomass and coal under oxy-fuel condition. *Int J Energy Res*. 2018;42(13):41 70-4183.

44. Gubba SR, Ingham DB, Larsen KJ, et al. Numerical modelling of the co-firing of pulverised coal and straw in a 300 MWe tangentially fired boiler. *Fuel Process Technol*. 2012;104:181-188.

45. Narayanan KV, Natarajan E. Experimental studies on cofiring of coal and biomass blends in India. *Renew Energy*. 2007;32 (15):2548-2558.

46. Kazagic A, Smajevic I. Experimental investigation of ash behavior and emissions during combustion of Bosnian coal and biomass. *Energy*. 2007;32(10):2006-2016.

47. Gil MV, Riaza J, Álvarez L, Pevida C, Pis JJ, Rubiera F. Kinetic models for the oxy-fuel combustion of coal and coal/biomass blend chars obtained in N_2 and CO_2 atmospheres. *Energy*. 2012;48(1):510-518.

48. Steer J, Marsh R, Griffiths A, Malmgren A, Riley G. Biomass co-firing trials on a down-fired utility boiler. *Energ Conver Manage*. 2013;66:285-294.

49. Wu H, Pedersen AJ, Glarborg P, Frandsen FJ, Dam-Johansen K, Sander B. Formation of fine particles in co-combustion of coal and solid recovered fuel in a pulverized coal-fired power station. *Proc Combust Inst*. 2011;33(2):2845-2852.

50. Zhuo J, Li S, Duan L, Yao Q. Effect of phosphorus transformation on the reduction of particulate matter formation during co-combustion of coal and sewage sludge. *Energy Fuel*. 2012; 26(6):3162-3166.

51. Nzihou A, Stanmore BR. The formation of aerosols during the co-combustion of coal and biomass. *Waste and Biomass Valorization*. 2015;6(6):947-957.

52. Wang X, Hu Z, Wang G, et al. Influence of coal co-firing on the particulate matter formation during pulverized biomass combustion. *J Energy Inst*. 2018;1-9.

53. Al-Naiema I, Estillore AD, Mudunkotuwa IA, Grassian VH, Stone EA. Impacts of co-firing biomass on emissions of particulate matter to the atmosphere. *Fuel*. 2015;162:111-120.

54. Wolski N, Maier J, Hein KRG. Fine particle formation from co-combustion of sewage sludge and bituminous coal. *Fuel Process Technol*. 2004;85(6-7):673-686.

55. Ndibe C, Maier J, Scheffknecht G. Combustion, cofiring and emissions characteristics of torrefied biomass in a drop tube reactor. *Biomass Bioenergy*. 2014;79:105-115.

56. Vekemans O, Laviolette JP, Chaouki J. Co-combustion of coal and waste in pulverized coal boiler. *Energy*. 2016;94:742-754.

57. Niu Y, Tan H, Hui S. Ash-related issues during biomass combustion: alkali-induced slagging, silicate melt-induced slagging (ash fusion), agglomeration, corrosion, ash utilization, and related countermeasures. *Prog Energy Combust Sci*. 2016; 52:1-61.

58. Kurose R, Ikeda M, Makino H. Combustion characteristics of high ash coal in a pulverized coal combustion. *Fuel*. 2001;80 (10):1447-1455.

59. Beckmann AM, Mancini M, Weber R, Seebold S, Müller M. Measurements and CFD modeling of a pulverized coal flame with emphasis on ash deposition. *Fuel*. 2016;167:168-179.

60. Jayanti S, Maheswaran K, Saravanan V. Assessment of the effect of high ash content in pulverized coal combustion. *App Math Model*. 2007;31(5):934-953.

61. Laxminarayan Y, Arendt P, Wu H, Jappe F, Sander B, Glarborg P. Biomass fly ash deposition in an entrained flow reactor. *Proc Combust Inst*. 2018;000:1-8.

62. Viskanta R, Menguc MP. Radiation heat transfer in combustion systems. *Prog Energy Combust Sci*. 1987;13(2):97-160.

63. Cai L, Zou C, Liu Y, Zhou K, Han Q, Zheng C. Numerical and experimental studies on the ignition of pulverized coal in O_2/H_2O atmospheres. *Fuel*. 2015;139:198-205.

64. Hashimoto N, Watanabe H. Numerical analysis on effect of furnace scale on heat transfer mechanism of coal particles in pulverized coal combustion field. *Fuel Process Technol*. 2016; 145(1):20-30.

65. Yu J, Zhang MC, Zhang J. Experimental and numerical investigations on the interactions of volatile flame and char combustion of a coal particle. *Proc Combust Inst*. 2009;32(2): 2037-2042.

66. Kumar M, Sahu SG. Study on the effect of the operating condition on a pulverized coal-fired furnace using computational fluid dynamics commercial code. *Energy Fuel*. 2007;21(6): 3189-3193.

67. Crnomarkovic N, Sijercic M, Belosevic S, Tucakovic D, Zivanovic T. Radiative heat exchange inside the pulverized lignite fired furnace for the gray radiative properties with thermal equilibrium between phases. *Int J Therm Sci*. 2014;85:21-28.

68. Chakraborty S, Rajora A, Singh SP, Talukdar P. Heat transfer and discrete phase modelling of coal combustion in a pusher type reheating furnace. *Appl Therm Eng*. 2017;116:66-78.

69. Zhang X, Yuan J, Chen Z, Tian Z, Wang J. A dynamic heat transfer model to estimate the flue gas temperature in the horizontal flue of the coal- fired utility boiler. *Appl Therm Eng*. 2018;135:368-378.

70. Inc. Ansys. Ansys Fluent Theory Guide.

71. Sadiki A, Agrebi S, Chrigui M, et al. Analyzing the effects of turbulence and multiphase treatments on oxy-coal combustion process predictions using LES and RANS. *Chem Eng Sci*. 2017; 166:283-302.

72. Kangwanpongpan T, Corrêa da Silva R, Krautz HJ. Prediction of oxy-coal combustion through an optimized weighted sum of gray gases model. *Energy*. 2012;41(1):244-251.

73. Sankar G, Kumar DS, Balasubramanian KR. Computational modeling of pulverized coal fired boilers—a review on the current position. *Fuel*. 2019;236:643-665.

74. Wu L, Qiao Y, Yao H. Experimental and numerical study of pulverized bituminous coal ignition characteristics in O_2/N_2 and O_2/CO_2 atmospheres. *Asia-Pac J Chem Eng*. 2012;7: 195-200.

75. Warzecha P, Boguslawski A. LES and RANS modeling of pulverized coal combustion in swirl burner for air and oxy-combustion technologies. *Energy*. 2014;66:732-743.

76. Gaikwad P, Kulkarni H, Sreedhara S. Simplified numerical modelling of oxy-fuel combustion of pulverized coal in a swirl burner. *Appl Therm Eng*. 2017;124:734-745.

77. Franchetti BM, Cavallo Marincola F, Navarro-Martinez S, Kempf AM. Large eddy simulation of a pulverised coal jet flame. *Proc Combust Inst*. 2013;34(2):2419-2426.

78. Ahn S, Tanno K, Watanabe H. Numerical analysis of particle dispersion and combustion characteristics on a piloted coaxial pulverized coal jet flame. *Appl Therm Eng*. 2017;124:1194-1202.

79. Bonefacic I, Frankovic B, Kazagic A. Cylindrical particle modelling in pulverized coal and biomass co-firing process. *Appl Therm Eng*. 2015;78:74-81.

80. Purimetla A, Cui J. CFD studies on burner secondary airflow. *App Math Model*. 2009;33(2):1126-1140.

81. Madejski P. Numerical study of a large-scale pulverized coal-fired boiler operation using CFD modeling based on the probability density function method. *Appl Therm Eng*. 2018;14 5:352-363.

82. Som SK, Mondal SS, Dash SK. Energy and exergy balance in the process of pulverized coal combustion in a tubular combustor. *J Heat Transfer*. 2005;127(12):1322.

83. Mondal SS. Modelling of transport processes and associated thermodynamic irreversibilities in ignition and combustion of a pulverized coal particle. *Int J Therm Sci*. 2008;47(11):14 42-1453.

84. Som SK, Sharma NY. Energy and exergy balance in the process of spray combustion in a gas turbine combustor. *J Heat Transfer*. 2002;124(5):828.

85. Som SK, Datta A. Thermodynamic irreversibilities and exergy balance in combustion processes. *Prog Energy Combust Sci*. 2008;34(3):351-376.

86. Xiong J, Zhao H, Zheng C. Exergy analysis of a 600 MWe oxy-combustion pulverized-coal-fired power plant. *Energy Fuel*. 2011;25(8):3854-3864.

87. Wang D, Chen S, Xu C, Xiang W. Energy and exergy analysis of a new hydrogen-fueled power plant based on calcium looping process. *Int J Hydrogen Energy*. 2013;38(13):5389-5400.

88. Wang L, Karimi N, Sutardi T, Paul MC. Numerical modelling of unsteady transport and entropy generation in oxy-combustion of single coal particles with varying fl ow velocities and oxygen concentrations. *Appl Therm Eng*. 2018;144:147-164.

89. Baum MM, Street PJ. Predicting the combustion behaviour of coal particles. *Combust Sci Technol*. 1971;3(5):231-243.

90. Badzioch S, Hawksley P. Kinetics of thermal decomposition of pulverized coal particles. *Ind Eng Chem Process Des Dev*. 1970; 9(4):521-530.

91. Kobayashi H, Howard JB, Sarofim AF. Coal devolatilization at high temperatures. *Symp Combust*. 1977;16(1):411-425.

92. Ubhayakar SK, Stickler DB, Von Rosenberg CW, Gannon RE. Rapid devolatilization of pulverized coal in hot combustion gases. *Symp Combust*. 1977;16(1):427-436.

93. Niksa S. FLASHCHAIN theory for rapid coal devolatilization kinetics. 4. Predicting ultimate yields from ultimate analyses alonE. *Energy Fuel*. 1994;8(3):659-670.

94. Fletcher TH, Kerstein AR, Pugmire RJ, Grant DM. Chemical percolation model for devolatilization. 2. Temperature and heating rate effects on product yields. *Energy Fuel*. 1990;4 (1):54-60.

95. Fletcher TH, Kerstein AR, Pugmire RJ, Solum MS, Grant DM. Chemical percolation model for devolatilization. direct use of 13C NMR data to predict effects of coal type. *Energy Fuel*. 1992;6(10):414-431.

96. Grant DM, Pugmire RJ, Fletcher TH, Kerstein AR. Chemical model of coal devolatilization using percolation lattice statistics. *Energy Fuel*. 1989;3(2):175-186.

97. Douglas Smoot L, Smith PJ. No_x pollutant formation in turbulent coal systems 1985;10:373−374.

98. Solomon PR, Fletcher TH. Impact of coal pyrolysis on combustion. *Symp Combust*. 1994;25(1):463-474.

99. Goshayeshi B, Sutherland JC. A comparison of various models in predicting ignition delay in single-particle coal combustion. *Combust Flame*. 2014;161(7):1900-1910.

100. Zou C, Cai L, Zheng C. Numerical research on the homogeneous/heterogeneous ignition process of pulverized coal in oxy-fuel combustion. *Int J Heat Mass Transf*. 2014; 73:207-216.

101. Richards AP, Fletcher TH. A comparison of simple global kinetic models for coal devolatilization with the CPD model. *Fuel*. 2016;185:171-180.

102. Lee H, Choi S. An observation of combustion behavior of a single coal particle entrained into hot gas flow. *Combust Flame*. 2015;162(6):2610-2620.

103. Khatami R, Stivers C, Levendis YA. Ignition characteristics of single coal particles from three different ranks in O_2/N_2 and O_2/CO_2 atmospheres. *Combust Flame*. 2012;159(12):3554-3568.

104. Bejarano PA, Levendis YA. Single-coal-particle combustion in O_2/N_2 and O_2/CO_2 environments. *Combust Flame*. 2008; 153(1-2):270-287.

105. Zhou H, Li Y, Li N, Cen K. Experimental investigation of ignition and combustion characteristics of single coal and biomass particles in O_2/N_2 and O_2/H_2O. *J Energy Inst*. 2018;1-10.

106. Hecht ES, Shaddix CR, Molina A, Haynes BS. Effect of CO_2 gasification reaction on oxy-combustion of pulverized coal char. *Proc Combust Inst*. 2011;33(2):1699-1706.

107. Hecht ES, Shaddix CR, Geier M, Molina A, Haynes BS. Effect of CO2and steam gasification reactions on the oxy-combustion of pulverized coal char. *Combust Flame*. 2012; 159(11):3437-3447.

108. Niu Y, Shaddix CR. A sophisticated model to predict ash inhibition during combustion of pulverized char particles. *Proc Combust Inst*. 2015;35(1):561-569.

109. Niu Y, Wang S, Shaddix CR, Hui S. Kinetic modeling of the formation and growth of inorganic nano-particles during pulverized coal char combustion in O_2/N_2 and O_2/CO_2 atmospheres. *Combust Flame*. 2016;173:195-207.

110. Niu Y, Liu X, Wang S, Hui S, Shaddix CR. A numerical investigation of the effect of flue gas recirculation on the evolution of ultra-fine ash particles during pulverized coal char combustion. *Combust Flame*. 2017;184:1-10.

111. Sun JK, Hurt RH. Mechanisms of extinction and near-extinction in pulverized solid fuel combustion. *Proc Combust Inst*. 2000;28(2):2205-2213.

112. Kim D, Choi S, Shaddix CR, Geier M. Effect of CO_2 gasification reaction on char particle combustion in oxy-fuel conditions. *Fuel*. 2014;120:130-140.

113. Niu Y, Liu S, Yan B, Wang S, Zhang X, Hui S. Effects of CO_2 gasification reaction on the combustion of pulverized coal char. *Fuel*. 2018;233:77-83.

114. Gonzalo-Tirado C, Jiménez S, Ballester J. Gasification of a pulverized sub-bituminous coal in CO_2 at atmospheric pressure in an entrained flow reactor. *Combust Flame*. 2012;159(1): 385-395.

115. Geier M, Shaddix CR, Davis KA, Shim HS. On the use of single-film models to describe the oxy-fuel combustion of pulverized coal char. *Appl Energy*. 2012;93:675-679.

116. Huang X, Pi LG, Liu Z, et al. Burnout characteristic of coal chars under oxyfuel combustion conditions. *Journal Eng Thermophys*. 2015;36(2):441-444.

117. Smith IW. The combustion rates of coal chars: a review. *Nineteenth Symposium on Combustion*. 1982;19(1):1045-1065. https://doi.org/10.1016/S0082-0784(82)80281-6.

118. Hurt RH, Sun JK, Lunden M. A kinetic model of carbon burnout in pulverized coal combustion. *Combust Flame*. 1998;113(1-2): 181-197.

119. Moroń W, Rybak W. NO_x and SO_2 emissions of coals, biomass and their blends under different oxy-fuel atmospheres. *Atmos Environ*. 2015;116:65-71.

120. Backreedy RI, Jones JM, Ma L, et al. Prediction of unburned carbon and NO_x in a tangentially fired power station using single coals and blends. *Fuel*. 2005;84(17):2196-2203.

121. Chen JC, Liu ZS, Huang JS. Emission characteristics of coal combustion in different O_2/N_2, O_2/CO_2 and O_2/RFG atmosphere. *J Hazard Mater*. 2007;142(1-2):266-271.

122. Hu YQ, Kobayashi N, Hasatani M. Effects of coal properties on recycled-NO_x reduction in coal combustion with O_2/recycled flue gas. *Energ Conver Manage*. 2003;44(14):2331-2340.

123. Belošević SV, Tomanović ID, Crnomarković ND, Milićević AR. Modeling of pulverized coal combustion for in-furnace NO_x reduction and flame control. *Therm Sci*. 2016;20:597-615.

124. Adamczyk WP, Werle S, Ryfa A. Application of the computational method for predicting NO_x reduction within large scale coal-fired boiler. *Appl Therm Eng*. 2014;73(1):343-350.

125. Bohnstein M, Langen J, Frigge L, Stroh A, Ströhle J, Epple B. Comparison of CFD simulations with measurements of gaseous sulfur species concentrations in a pulverized coal fired 1 MW_{th} furnace. *Energy Fuel*. 2016;30(11):9836-9849.

126. Costa M, Silva P, Azevedo JLT. Measurements of gas species, temperature, and char burnout in a low-NO_x pulverized-coal-fired utility boiler. *Combust Sci Technol*. 2003;175(2):271-289.

127. Ribeirete A, Costa M. Impact of the air staging on the performance of a pulverized coal fired furnace. *Proc Combust Inst*. 2009;32(2):2667-2673.

128. Shen J, Liu J, Zhang H, Jiang X. NO_x emission characteristics of superfine pulverized anthracite coal in air-staged combustion. *Energ Conver Manage*. 2013;74:454-461.

129. Chen Z, Wang Z, Li Z, Xie Y, Ti S, Zhu Q. Experimental investigation into pulverized-coal combustion performance and NO formation using sub-stoichiometric ratios. *Energy*. 2014;73:8 44-855.

130. Wielgosinski G, Łechtanska P, Namiecinska O. Emission of some pollutants from biomass combustion in comparison to hard coal combustion. *J Energy Inst*. 2016;1-10.

131. Miller BG.. *Coal Energy Systems*. 2004.

132. Zaman M, Lee JH. Carbon capture from stationary power generation sources: a review of the current status of the technologies. *Korean J Chem Eng*. 2013;30(8):1497-1526.

133. Mondal MK, Balsora HK, Varshney P. Progress and trends in CO_2 capture/separation technologies: a review. *Energy*. 2012;46(1):431-441.

134. Zou C, Cai L, Wu D, Liu Y, Liu S, Zheng C. Ignition behaviors of pulverized coal particles in O_2/N_2 and O_2/H_2O mixtures in a drop tube furnace using flame monitoring techniques. *Proc Combust Inst*. 2015;35(3):3629-3636.

135. Pettinau A, Ferrara F, Amorino C. Combustion vs. gasification for a demonstration CCS (carbon capture and storage) project in Italy: a techno-economic analysis. *Energy*. 2013;50(1):1 60-169.

136. Escudero AI, Espatolero S, Romeo LM, et al. Minimization of CO_2 capture energy penalty in second generation oxy-fuel power plants. *Appl Therm Eng*. 2016;103:274-281.

137. Cormos C. Oxy-combustion of coal, lignite and biomass: a techno-economic analysis for a large scale Carbon Capture and Storage (CCS) project in Romania. *Fuel*. 2016;169:50-57.

138. Soundararajan R, Gundersen T. Coal based power plants using oxy-combustion for CO_2 capture: pressurized coal combustion to reduce capture penalty. *Appl Therm Eng*. 2013;61(1):115-122.

139. Garg A, Shukla PR, Parihar S, Singh U, Kankal B. Cost-effective architecture of carbon capture and storage (CCS) grid in India. *Int J Greenh Gas Control*. 2017;66:129-146.

140. Hu Y, Li H, Yan J. Integration of evaporative gas turbine with oxy-fuel combustion for carbon dioxide capture. *Int J Green Energy*. 2010;7(6):615-631.

141. Amrollahi Z, Ertesvåg IS, Bolland O. Thermodynamic analysis on post-combustion CO_2 capture of natural-gas-fired power plant. *Int J Greenh Gas Control*. 2011;5(3):422-426.

142. BP Statistical Review of World Energy 67th edition 2018.

143. Chen X, Xie J, Mei S, He F. NO_x and SO_2 Emissions during co-combustion of RDF and anthracite in the environment of precalciner. *Energies*. 2018;11(2):337-350.

144. Badour C, Gilbert A, Xu C, et al. Combustion and air emissions from co-firing a wood biomass, a Canadian peat and a Canadian lignite coal in a bubbling fluidised bed combustor. *Can J Chem Eng*. 2012;90(5):1170-1177.

145. Nussbaumer T. Combustion and co-combustion of biomass: fundamentals, technologies, and primary measures for emission reduction. *Energy Fuel*. 2003;17(6):1510-1521.

146. Wang X, Hu Z, Deng S, Xiong Y, Tan H. Effect of biomass/coal co-firing and air staging on NO_x emission and combustion efficiency in a drop tube furnace. *Energy Procedia*. 2014;61: 2331-2334.

147. Ti S, Chen Z, Kuang M, et al. Numerical simulation of the combustion characteristics and NO_x emission of a swirl burner: Influence of the structure of the burner outlet. *Appl Therm Eng*. 2016;104:565-576.

148. Khaldi N, Chouari Y, Mhiri H, Bournot P. CFD investigation on the flow and combustion in a 300 MWe tangentially fired pulverized-coal furnace. 2016:1881−1890.

149. Tu Y, Liu H, Chen S, Liu Z, Zhao H, Zheng C. Numerical study of combustion characteristics for pulverized coal under oxy-MILD operation. *Fuel Process Technol*. 2015;135:80-90.

150. Guo J, Liu Z, Wang P, et al. Numerical investigation on oxy-combustion characteristics of a 200 MWetangentially fired boiler. *Fuel*. 2015;140:660-668.

151. Rebola A, Azevedo JLT. Modelling coal combustion with air and wet recycled flue gas as comburent in a 2.5 MWth furnace. *Appl Therm Eng*. 2015;86:168-177.

152. Cai J, Handa M, Modest MF. Eulerian-Eulerian multi-fluid methods for pulverized coal flames with nongray radiation. *Combust Flame*. 2015;162(4):1550-1565.

153. Du Y, Wang C, Lv Q, Li D, Liu H, Che D. CFD investigation on combustion and NOxemission characteristics in a 600 MW wall-fired boiler under high temperature and strong reducing atmosphere. *Appl Therm Eng*. 2017;126:407-418.

154. Heil P, Toporov D, Förster M, Kneer R. Experimental investigation on the effect of O_2 and CO_2 on burning rates during oxyfuel combustion of methane. *Proc Combust Inst*. 2011;33 (2):3407-3413.

155. Kim RG, Li D, Jeon CH. Experimental investigation of ignition behavior for coal rank using a flat flame burner at a high heating rate. *Exp Therm Fluid Sci*. 2014;54:212-218.

156. Weidmann M, Honoré D, Verbaere V, et al. Experimental characterization of pulverized coal MILD flameless combustion from detailed measurements in a pilot-scale facility. *Combust Flame*. 2016;168:365-377.

157. Zellagui S, Schönnenbeck C, Zouaoui-Mahzoul N, et al. Pyrolysis of coal and woody biomass under N_2 and CO_2 atmospheres using a drop tube furnace—experimental study and kinetic modeling. *Fuel Process Technol*. 2016;148:99-109.

158. Maffei T, Khatami R, Pierucci S, Faravelli T, Ranzi E, Levendis YA. Experimental and modeling study of single coal particle combustion in O_2/N_2 and Oxy-fuel (O_2/CO_2) atmospheres. *Combust Flame*. 2013;160(11):2559-2572.

159. Modliński N, Madejski P, Janda T, Szczepanek K, Kordylewski W. A validation of computational fluid dynamics temperature distribution prediction in a pulverized coal boiler with acoustic temperature measurement. *Energy*. 2015;92:77-86.

160. Tamura M, Watanabe S, Kotake N, Hasegawa M. Grinding and combustion characteristics of woody biomass for co-firing with coal in pulverised coal boilers. *Fuel*. 2014;134: 544-553.

161. Sahu SG, Mukherjee A, Kumar M, et al. Evaluation of combustion behaviour of coal blends for use in pulverized coal injection (PCI). *Appl Therm Eng*. 2014;73(1):1012-1019.

162. Marek E, Świątkowski B. Experimental studies of single particle combustion in air and different oxy-fuel atmospheres. *Appl Therm Eng*. 2014;66(1-2):35-42.

163. Magdziarz A, Wilk M. Thermogravimetric study of biomass, sewage sludge and coal combustion. *Energ Conver Manage*. 2013;75:425-430.

164. Moghtaderi B. A study on the char burnout characteristics of coal and biomass blends. *Fuel*. 2007;86(15):2431-2438.

165. Meesri C, Moghtaderi B. Experimental and numerical analysis of sawdust-char combustion reactivity in a drop tube reactor. *Combust Sci Technol*. 2003;175(4):793-823.